

**MICROBIAL COMMUNITY RESPONSE TO PERMAFROST THAW IN THE  
CANADIAN HIGH ARCTIC**

2024 | CHLOE BARBARA MACLEAN

B.Sc. HONOURS THESIS – BIOLOGY



**MICROBIAL COMMUNITY RESPONSE TO PERMAFROST THAW IN THE  
CANADIAN HIGH ARCTIC**

by

CHLOE BARBARA MACLEAN

A THESIS SUBMITTED IN PARTIAL FULFILLMENT  
OF THE REQUIREMENTS FOR THE DEGREE OF

BACHELOR OF SCIENCE (HONS.)

in the

DEPARTMENT OF BIOLOGICAL SCIENCES

Ecology and Environmental Biology



**THOMPSON RIVERS UNIVERSITY**

This thesis has been accepted as conforming to the required standards by:

Eric Bottos (Ph.D.), Thesis Supervisor, Dept. Biological Sciences

Jonathan Van Hamme (Ph.D.), Co-supervisor, Dept. Biological Sciences

Matthew Reudink (Ph.D.), External examiner, Dept. Biological Sciences

Dated this 10<sup>th</sup> day of April 2024, in Kamloops, British Columbia, Canada

© Chloe Barbara MacLean, 2024

## ABSTRACT

Permafrost is one of Earth's most crucial carbon reservoirs, as the perennially frozen state of permafrost protects stored carbon from microbial metabolisms. Increasing surface temperatures are causing the permafrost to thaw, making permafrost carbon more bioavailable to microbial processes, which can transform this newly available carbon to greenhouse gases such as methane and carbon dioxide. Permafrost thaw additionally shifts the environmental conditions of the newly thawed soil, which changes the selective pressures that shape the microbial community composition. The active layer, which is exposed to seasonal freezing and thawing cycles, lies above the permafrost and contains a microbial community that differs in composition compared to the permafrost microbial community. Thawing of the permafrost induces the mixing of the permafrost and active layer communities, as well as the mixing of the nutrients between these two layers. How the changes in selective pressures, the mixing of nutrients, and the mixing of microbial communities affect the microbial community composition in the newly thawed soil is not well understood. This study examined the microbial community response to permafrost thaw using soil samples collected from two field sites in the Canadian High Arctic, near Cambridge Bay, Nunavut: Long Point and Augustus Hills. Treatments were designed to evaluate the importance of two factors that influence microbial community assembly processes during thaw: microbial dispersal and shifting selective pressures that accompany permafrost thaw. Microcosms of permafrost and active layer soil samples were established in sterile serum bottles and incubated at 8 °C for up to 5 months. The influence of nutrient mixing on post-thaw microbial community composition was examined by the addition of nutrients extracted from one soil layer to a microcosm containing soil of the opposite layer, while the influence of microbial dispersal on microbial community composition following thaw was investigated by inoculating each soil type with soil from the opposite layer. The collective influence of nutrient mixing and microbial dispersal on microbial community composition following permafrost thaw was examined by adding both the extracted nutrients and the soil inoculum from one soil type to the opposite soil type. As a control, the effects of the changing selective pressures associated with thaw on the permafrost microbial community composition and the active layer microbial community composition were examined without the influence of nutrient mixing or microbial dispersal. Samples were taken monthly and changes in the microbial community composition were assessed by 16S rRNA gene amplicon sequencing. The microbial community compositions differed significantly between the two field sites (permafrost:

$\Pr(>F) = 0.011$ ; active layer:  $\Pr(>F) = 0.003$ ). The results of the Augustus Hills microcosms showed consistent shifts in microbial community composition following thaw, which indicates that the selective pressures induced by thaw are important drivers of shifts in microbial community composition following permafrost thaw. The results of the Long Point microcosms showed consistent shifts in microbial community composition only in the active layer-dominant microcosms. The Long Point permafrost-dominant microcosms showed no consistent shifts following permafrost thaw; however, these were the only microcosms that showed that microbial dispersal had a stronger influence on post-thaw microbial community composition than the selective pressures associated with thaw. The results suggest that the change in selective pressures that accompany permafrost thaw are the most important ecological factors that influence post-thaw microbial community composition, and that initial microbial community composition is an important factor in determining microbial community composition following permafrost thaw. The heterogeneity observed in community composition and in response to thaw between sites indicates that extrapolating results from a limited range of sites is highly problematic, and therefore many areas need to be studied to understand the response to permafrost thaw across the Canadian High Arctic.

Thesis Supervisor: Dr. Eric Bottos

## ACKNOWLEDGEMENTS

Having the privilege to complete this Honours project has been an incredibly rewarding experience that has undoubtedly shaped me into a better student, researcher, and person. I would like to express my deepest appreciation to my primary supervisor, Dr. Eric Bottos, whose guidance and unwavering support has been instrumental in the successful completion of this thesis. I am extremely grateful to my co-supervisor, Dr. Jonathan Van Hamme, who generously provided microbial expertise and bioinformatics skills. Additionally, special thanks to Dr. Louis Gosselin for serving as the Chair of my Thesis defence, and also for providing me with the amazing opportunity to become involved in research in 2022. I am very thankful for the mentoring I have received from these three inspiring individuals.

I'd like to acknowledge Dr. Matt Reudink, for serving as the External Examiner on my Thesis defence committee. I would also like to extend thanks to Breanne McAmmond, for her extensive assistance in the experiment set-ups, managing the sequencing of samples, and also for being a great moral support and friend. Lastly, I would like to thank the CHARS scientists who completed the sampling of the soils used in this project: Dr. Stephanie Coulombe, Dr. Ian Hogg, and Bryan Vandenbrink. Funding was provided by a NSERC-USRA award to myself, and an NSERC Discovery grant to Dr. Eric Bottos.

## TABLE OF CONTENTS

TABLE OF CONTENTS .....	v
1. INTRODUCTION.....	1
2. METHODS.....	5
2.1 Soil collection and processing.....	5
2.2 Soil incubations .....	7
2.2.1 Nutrient extraction.....	7
2.2.2 Microcosm preparation .....	7
2.2.3 Maintenance of microcosms.....	10
2.3 Sampling of microcosms .....	11
2.3.1 DNA extraction .....	11
2.3.2 Library preparation.....	11
2.3.3 16S rRNA gene sequencing and data processing .....	12
2.4 Data analysis .....	13
3. RESULTS.....	14
3.1 Characterizing microbial community composition at two field sites in the Canadian High Arctic .....	14
3.2 The effect of permafrost thaw on microbial community composition .....	17
3.2.1 The influence of microbial dispersal and nutrient inputs on the post-thaw microbial community composition of the Long Point samples .....	19
3.2.2 The influence of microbial dispersal and nutrient inputs on the post-thaw microbial community composition of the Augustus Hills samples. ....	22
4. DISCUSSION .....	25
4.1 Characterizing microbial community composition at two field sites in the Canadian High Arctic .....	25
4.2 The effect of permafrost thaw on microbial community composition .....	26
4.2.1 The influence of microbial dispersal and nutrient inputs on the post-thaw microbial community composition of the Long Point samples .....	26
4.2.2 The influence of microbial dispersal and nutrient inputs on the post-thaw microbial community composition of the Augustus Hills samples. ....	27
4.3 Conclusions .....	28
5. LITERATURE CITED .....	30
6. APPENDIX .....	35

## LIST OF FIGURES

Figure 1. Field sites near Cambridge Bay, Nunavut: Augustus Hills (AH) and Long Point (LP). ...	6
Figure 2. Schematic diagram representing the experimental design that was used for the replicate experiments (Augustus Hills and Long Point) with four categories of treatments, each containing two treatments. Microcosms were extracted in triplicate at each of the five timepoints shown in weeks. ....	8
Figure 3. Schematic diagram representing the microcosms associated with the Long Point (A) and Augustus Hills experiments (B) as a result of the complications that arose during experiment set up. ....	10
Figure 4. Manifold setup used to purge eight microcosms at a time. ....	11
Figure 5. Relative abundances of phyla observed in the permafrost and active layer microcosms at Time 0 for both field sites. The “OTHER” category represents grouped phyla that each made up less than 1% of every sample. ....	15
Figure 6. MDS Plot representing the Bray-Curtis dissimilarity in microbial community composition between the microcosms containing active layer or permafrost soil at Time 0 for both the Long Point and Augustus Hills field sites. ....	16
Figure 7. Relative abundances of phyla observed in the Long Point (A) and Augustus Hills (B) experimental microcosms. The “OTHER” category represents grouped phyla that each made up less than 1% of every sample. Missing samples were either not created due to complications in experiment set up or were removed from analysis due to having fewer than 10,000 reads. ....	18
Figure 8. MDS Plots representing the Bray-Curtis dissimilarity in microbial community composition between (A) all Long Point treatments microcosms, (B) active layer-dominant Long Point microcosms, and (C) permafrost-dominant Long Point microcosms. ....	20
Figure 9. MDS Plots representing the Bray-Curtis dissimilarity in microbial community composition between (A) all Augustus Hills treatments microcosms, (B) active layer-dominant Augustus Hills microcosms, and (C) permafrost-dominant Augustus Hills microcosms. ....	23

## 1. INTRODUCTION

The Arctic occupies the northernmost region of Earth and is most commonly defined as the portion of both land and water that is within the Arctic Circle: a latitude line of about 66°34'N. The Arctic region spans Asia, Europe and North America, with eight countries containing land within the Arctic Circle: Canada, the United States, Denmark, Iceland, Norway, Sweden, Finland and Russia. Gradients in environmental conditions have allowed ecologists to divide terrestrial Arctic ecosystems into three biogeographical zones: the High Arctic, the Low Arctic, and the Subarctic (Jones et al., 2009). Together the Arctic and the Subarctic make up the Circumpolar region. Low temperatures, severe weather conditions, and extended durations of light and darkness contribute to the Arctic being characterized as one of Earth's extreme environments. This makes the Arctic an interesting environment for studying the ecology and evolution of microbial life that is adapted to the extreme conditions (Rampelotto, 2014). In terms of temperature, the Arctic can be defined as the region north of the 10°C July isotherm. Generally considered an extreme environment, there is significant spatial and temporal variation in temperature, precipitation, UV radiation, vegetation, and soil characteristics across the Arctic (Rampelotto, 2014).

Arctic soils represent one unique element of Arctic environments, often containing multiple distinct soil horizons and being affected by cryogenic processes such as cryoturbation (Bockheim, 2007). Approximately 27% of Circumpolar region soils are classified as cryosols: mineral or organic material affected by permafrost (Jones et al., 2009). Permafrost is defined as the earth material that has remained frozen for a minimum of two consecutive years (Schuur et al., 2008). Approximately 16% of the global soil area is composed of permafrost (Tarnocai et al., 2008); permafrost can be found from 26°N in the Himalayas to 85°N in Greenland, with approximately 70% of the permafrost occurring between 45°N and 67°N (Zhang et al., 1999). Variation exists in the spatial distribution of permafrost, ranging from continuous permafrost (91-100% coverage) to isolated patches of permafrost (<10% coverage) (Jones et al., 2009).

Typically, above the permafrost layer is the active layer, which freezes and thaws annually, and, during the summer months, can reach depths of 20-150 cm before refreezing in the winter (Jones et al., 2009). Microbial communities are found in both permafrost soil and active layer soil,

however communities residing in the permafrost layer inhabit an environment that is very different to that of the active layer: the permafrost layer is highly structured and microorganisms in this layer experience freezing temperatures, low water and nutrient availability, and high salinity levels (Mackelprang et al., 2016; Jansson and Tas, 2014). The active layer contains more biomass and a larger diversity of microorganisms than the permafrost layer (Mackelprang et al., 2016; Yergeau et al., 2010), reflecting the decreased microbial habitability of the permafrost layer relative to the active layer. Multiple studies have shown that microbial community structures differ between the permafrost layer and the active layer (Steven et al., 2008; Müller et al., 2018; Monteux et al., 2018), and permafrost microbes have been found to have reduced functional potential relative to microbes found in the active layer (Hultman et al., 2015). Cold-adapted microbes have evolved many strategies that help them survive and proliferate at low temperatures (D'Amico et al., 2006); for example, dormancy is a common survival strategy with both non-spore-forming and spore-forming bacteria being found in permafrost (Mackelprang et al., 2017; Liang et al., 2019). Besides dormancy, other survival strategies include horizontal gene transfer, which allows for the uptake of potentially advantageous genes, and stress response genes, which can increase the likelihood of survival under harsh environmental conditions (Mackelprang et al., 2017).

Permafrost soils represent one of Earth's largest carbon stores (Tarnocai et al., 2008; Schuur et al., 2008). The frozen conditions of the permafrost largely protect the stored carbon from microbial processes (Mackelprang et al., 2016); however, rising surface temperatures are causing the active layer to deepen, mobilizing the sequestered carbon and making it available to microbial metabolisms (Fox-Kemper et al., 2021). Over the period of 1979-2021, the Arctic warmed 3.8 times faster than the rest of the planet (Rantanen et al., 2022). Changing patterns of precipitation and frequent fire events can also influence permafrost degradation (Schuur et al., 2015). Carbon dioxide and other greenhouse gasses are produced as microbes decompose carbon, and these products significantly contribute to climate change (Mackelprang et al., 2011). Thus, the thawing of permafrost and the subsequent microbial degradation of stored carbon represents a potential significant positive feedback loop from terrestrial ecosystems to the atmosphere (Schuur et al., 2008).

In addition to the overarching global implications, the effects of Arctic permafrost thaw can also be observed at a regional level. Approximately 50% of Canada is underlain by permafrost (Jones et al., 2009), and warmer than average summer temperatures in the Canadian Arctic are causing the active layer to deepen (Farquharson et al., 2019). Models predict that by the year 2100 less than 10% of near-surface permafrost will remain (Lawrence and Slater, 2005). Communities that reside on permafrost in the Canadian Arctic are vulnerable to the changes inflicted by thawing permafrost including erosion, shifting vegetation and biomes, and reduced food security (Schuur and Mack, 2018); a study by Ramage et al. (2022) surveyed members of a community in the Canadian High Arctic and 87% of participants indicated that permafrost thaw has negatively impacted their lives in the last ten years (Ramage et al., 2022).

Despite the urgent need to better understand the composition and ecology of permafrost microbial communities, there is an underrepresentation of microbiology-related soil research in the Canadian Arctic (Metcalf et al., 2018). Previous Canadian microbiology studies have conducted metagenomic characterizations (Yergeau et al., 2010) and examined microbial diversity within the permafrost layer (Steven et al., 2007; Steven et al., 2008), however these studies are largely restricted to a limited number of permafrost cores (<5). To date, only two Canadian studies have correlated microbial community structure to variation in environmental conditions: a study by Saidi-Mehrabad et al. (2020) correlated changes in soil chemistry and microbial community composition in a single core with horizons originating from two epochs (temporal comparison). Varsadiya et al. (2021) examined microbial community structure in three field sites each occupying a different tundra type; this study found that both soil horizon and tundra type were significant factors affecting variation in bacterial community structure, with pH and total carbon being the most significant physicochemical parameters.

Previous studies have examined the effects of thaw on the microbial community within the permafrost alone (Allan et al., 2014; Qin et al., 2021), or on the microbial communities within permafrost and the active layer independently (Mackelprang et al., 2011; Chen et al., 2016; Adamczyk et al., 2021). However, there is a lack of research investigating how permafrost thaw will affect the microbial communities in the active layer and permafrost layer collectively once the dispersal and nutritional barriers between these two layers disappears. In-situ thaw experiments

have also been conducted to examine the changes in microbial community composition following thaw (Monteux et al., 2018), but these experiments are founded on the assumption that the physicochemical soil properties and pre-thaw microbial community composition are consistent across landscapes.

The main environmental factor that shapes the composition of permafrost microbial communities is dispersal limitation and the associated selective pressures generated by prolonged freezing (Bottos et al., 2018; Doherty et al., 2020); thus, diversification through mutation followed by natural selection is the dominant mechanism by which available niches are occupied in permafrost soils and new members are introduced to microbial communities (Ernakovich et al., 2022). However, as permafrost thaws, constraints on microbial dispersal are relieved and populations are allowed to mix within the newly thawed permafrost and with the overlying active layer populations. Microbial dispersal is identified in the microbial community assembly theory as one way that new members can be introduced to a community (Vellend, 2010; Nemergut et al., 2013). An *in-situ* study conducted in Northern Sweden found that, while initial active layer and permafrost microbial communities differed strongly, post-thaw communities resembled the active layer community (Monteux et al., 2018); this suggests that active layer populations colonize newly thawed soil and out-compete the permafrost layer populations.

Another factor that has a strong influence on microbial community structure following permafrost thaw is increased nutrient availability (Ernakovich et al., 2022). The increased nutrient availability following thaw is reflected in rapid shifts in abundances of genes involved in carbon and nitrogen cycling that have been observed in permafrost microbial communities (Mackelprang et al., 2011). An increase in nutrient availability may negatively impact permafrost microbial populations in the newly thawed environment, as these microorganisms are adapted to the oligotrophic conditions of the permafrost environment. Therefore, this provides an opportunity for the active layer microbial community, which is pre-adapted to thrive in the thawed conditions, to out-compete members of the permafrost microbial community.

The purpose of this study is to examine how permafrost microbial community composition changes following permafrost thaw, and to resolve the primary ecological drivers of these changes.

Specifically, we (1) characterized the microbial community composition at two field sites in the Canadian High Arctic, and (2) determined how microbial dispersal and nutrient mixing between the permafrost and the active layer affect microbial community responses to permafrost thaw at these sites. Goal (1) aims to test the hypothesis that the initial active layer and permafrost microbial community compositions significantly differ from each other at each field site, and the two field sites differ from each other in their initial microbial community compositions. Goal (2) considers important ecological processes likely to occur following permafrost thaw: the change in selective pressures that result from permafrost thaw and microbial dispersal between permafrost and active layer communities. The influences of these processes on post-thaw microbial community composition were investigated independently and together. We hypothesize that microbial dispersal from the active layer to the permafrost will have a stronger influence on post-thaw microbial community composition than the changing selective pressures that accompany thaw (increased temperature, mixing of nutrients) alone, as active layer microbes will outcompete permafrost microbes in newly thawed soils. In contrast, we hypothesized that microbial dispersal from the permafrost to the active layer will not induce stronger shifts in community composition than the changing selective pressures that accompany thaw, as permafrost microbes are not well adapted to active layer conditions.

## **2. METHODS**

### *2.1 Soil collection and processing*

In August of 2023, soil samples were gathered from the Canadian High Arctic Research Station (CHARS), on the south coast of Victoria Island, Nunavut. Field sites located near CHARS were selected by a colleague of Dr. Bottos', Dr. Stephanie Coulombe. Permafrost cores and active layer samples were collected at two field sites: Augustus Hills (69°10'01" N, 105°38'01" W) and Long Point (69°07'29" N, 105°24'20" W) (Fig. 1). The permafrost cores and active layer samples were collected from Long Point during the summer of 2021, while the permafrost cores and active layer samples were collected from Augustus Hills during the summer of 2023.



Figure 1. Field sites near Cambridge Bay, Nunavut: Augustus Hills (AH) and Long Point (LP).

At both field sites, active layer soil samples were retrieved using a sterile trowel and placed in sterile sampling bags. Permafrost cores were retrieved using a gas-powered frozen soil auger, wrapped in aluminum foil, and placed in sampling bags. Active layer and permafrost soil samples were placed on ice and transported to CHARS, where they were stored at  $-20^{\circ}\text{C}$ .

Frozen cores were decontaminated as previously described in order to remove any non-permafrost material from the surface of the cores (Bottos et al., 2018). Briefly, cores were placed on sterile aluminum foil and struck with a sterile chisel to expose pristine surfaces at the top and bottom of the core; starting from these surfaces, a sterile razor blade was used to carefully chip away the outer surface along the length of the permafrost core, sterilizing the blade with ethanol and flame between strikes. The decontaminated cores were then placed in sterile bags and kept frozen until they were returned to the Microbial Ecology Laboratory at TRU.

## 2.2 Soil incubations

### 2.2.1 Nutrient extraction

Water-soluble nutrients were extracted prior to the creation of the microcosms by adding soil from either the permafrost core or the active layer samples to 18 mega $\Omega$  water in a 50-ml conical tube at a ratio of 1 g:2 ml. The solution was then shaken and left on ice for one hour, with shaking every 15 minutes. Following the one-hour period, the solution was vortexed at 3000 rpm for three minutes, before being vacuumed filtered through a filter with a pore size of 0.22  $\mu$ m. Once filtered, the water-soluble nutrient solutions were stored at 4°C until the microcosms were ready to receive the nutrient solutions.

### 2.2.2 Microcosm preparation

Thaw experiments were conducted simultaneously for the two field sites. In each experiment, sterile 60-ml serum bottles were used to establish microcosms each containing one of eight different treatments designed to mimic processes that are likely to occur following permafrost thaw (Fig. 2). The two control treatments include 10 g of permafrost soil only (PS) and 10 g of active layer soil only (AS), these treatments examine the individual responses to thaw of these two soil layers without the influence of microbial dispersal or nutrient inputs from the other layer. The dispersal treatments facilitate the introduction of the microorganisms in each soil type to the other soil type by mixing the two soil types: 9g:1g permafrost soil to active layer soil (PF+AM) and 9g:1g active layer soil to permafrost soil (AS+PM). The dispersal treatments examine the influence of microbial dispersal from the other soil layer on post-thaw microbial community composition. The nutrient treatments include the addition of 1 ml of the water-soluble nutrients extracted from the active layer soil to 10 g of permafrost soil (PS+AN), and the addition of 1 ml of the water-soluble nutrients extracted from the permafrost soil to 10 g of active layer soil (AS+PN). These nutrient treatments examine the effect of nutrient inputs from the other soil layer on post-thaw microbial community composition. Lastly, the dispersal + nutrients treatments combine the dispersal and nutrient treatments by adding 1 ml of active layer nutrients to a serum bottle containing 9g:1g permafrost soil to active layer soil (PS+AN+AM), and by adding 1 ml of permafrost nutrients to a serum bottle containing 9g:1g active layer soil to permafrost soil

(AS+PN+PM). The dispersal + nutrients treatments examine the combined effects of microbial dispersal and nutrient inputs from the other soil layer on microbial community composition following thaw. The four treatments that did not receive 1 ml of a water-soluble nutrient solution (PS, AS, PS+AM, and AS+PM) instead received 1 ml of 18 mega $\Omega$  water.

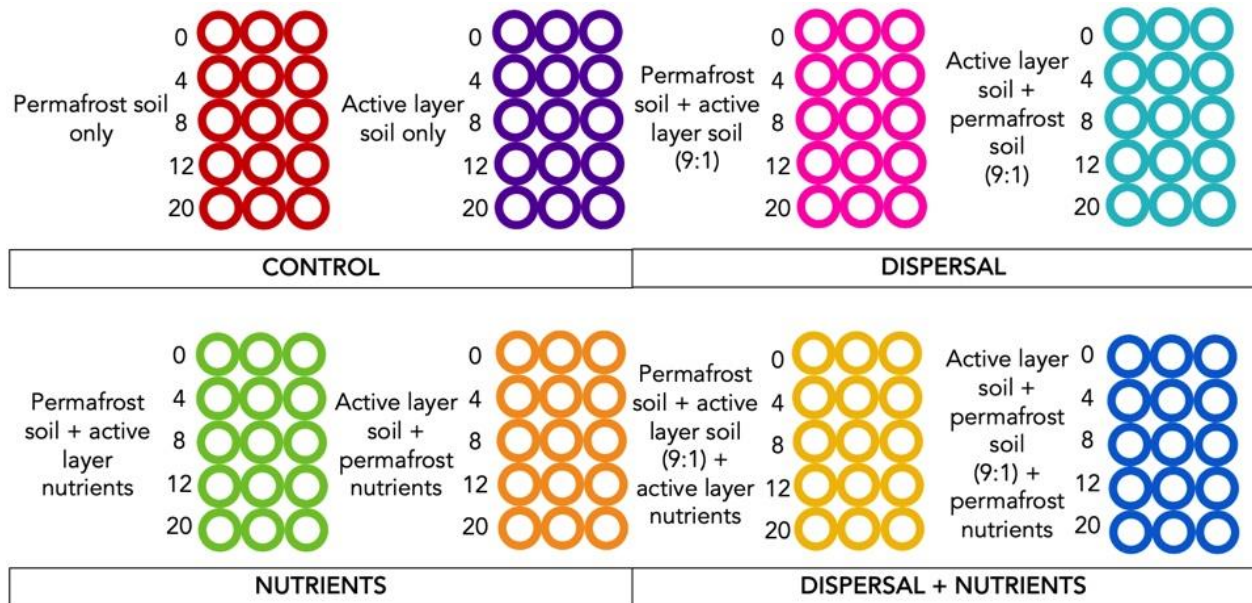


Figure 2. Schematic diagram representing the experimental design that was used for the replicate experiments (Augustus Hills and Long Point) with four categories of treatments, each containing two treatments. Microcosms were extracted in triplicate at each of the five timepoints shown in weeks.

Prior to the first day of experiment set up, the active layer samples and permafrost cores were thawed at 4°C overnight. Soil samples were then homogenized, and aseptic techniques were used to fill sterile serum bottles with the appropriate amounts of each soil type. All soil bags used during the set-up process were kept on ice and kept closed as long as possible. Soil microcosms were prepared using a sterile scoopula and stored at 4°C until all microcosms for that site had been prepared. All microcosms then received either 1 ml of a water-soluble nutrient solution or 1 ml of 18 mega $\Omega$  water, depending on the treatment. Sterile rubber stoppers were then placed in the bottle opening, followed by an aluminum cap which, after sealing with a crimping tool, made the microcosm airtight. Completed microcosms were then incubated at 8°C.

Minor changes to the experimental design were made due to complications that arose during the set-up of both the Long Point and Augustus Hills experiments. Regarding the Long Point experiment, the only complication that occurred was that 10 g of permafrost soil was added to the treatments that only required 9 g of permafrost soil (PS+AM and PS+AN+AM) (Fig. 3A). The Augustus Hills permafrost core had very high water content. To ensure that each microcosm received an equal amount of the permafrost sediment and the permafrost liquid, the two parts of the permafrost core were separated by pouring off the liquid into an autoclaved bottle. This process resulted in the permafrost sediment having a total mass of 417 g and the permafrost liquid having a total mass of 263 g. Using the ratio of mass of permafrost sediment: mass of permafrost liquid and assuming that 1 ml of permafrost liquid = 1 g, it was calculated that for the treatments that required 1 g of permafrost soil, 0.386 ml of permafrost liquid and 0.614 g of permafrost sediment was required; for the treatments that required 9 g of permafrost soil, 3.48 ml of permafrost liquid and 5.52 g of permafrost sediment was required; and for the treatments that required 10 g of permafrost soil, 3.86 ml of permafrost liquid and 6.14 g of permafrost sediment was required. Even with these adjustments, the permafrost sediment was depleted with two microcosms remaining to be filled; these two microcosms were removed from the PS+AN treatment. Additionally, both the permafrost nutrient solution and the active layer nutrient solution were depleted before all the microcosms were completed; this led to six of the PS+AN microcosms and six of the AS+PN microcosms lacking the addition of the nutrient solution. Since these issues left only seven microcosms for the PS+AN treatment, these microcosms were used for the 0-week timepoint (three microcosms) and for the 20-week timepoint (four microcosms); the nine remaining AS+PN microcosms were evenly divided between the 0-week (Time 0), 8-week, and 10-week timepoints (Fig. 3B).

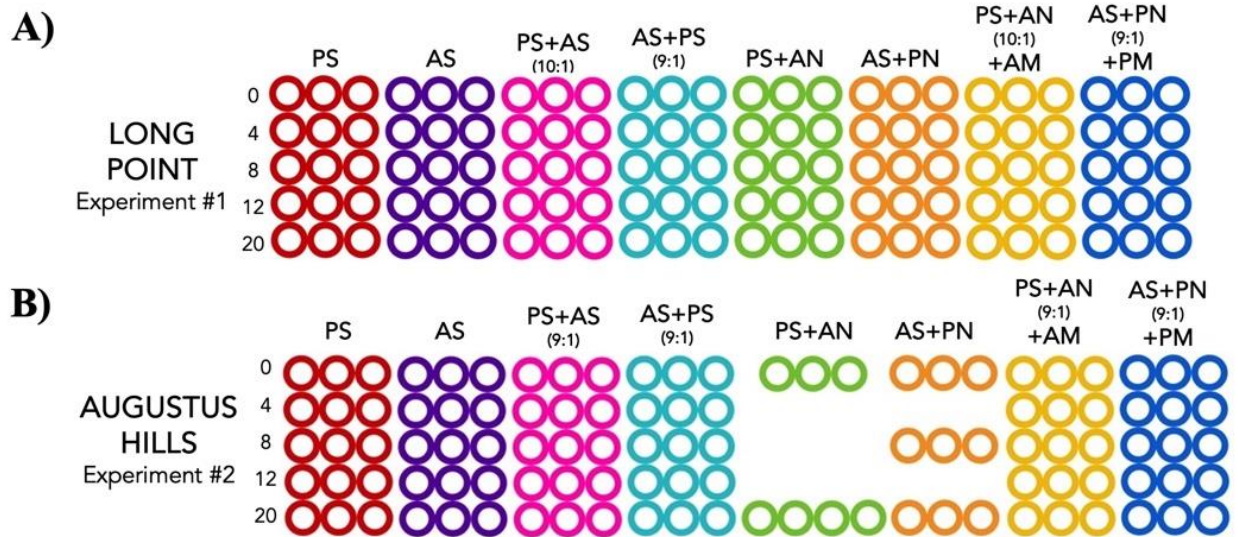


Figure 3. Schematic diagram representing the microcosms associated with the Long Point (A) and Augustus Hills experiments (B) as a result of the complications that arose during experiment set up.

### 2.2.3 Maintenance of microcosms

To maintain the aerobic environment within the airtight microcosms, each microcosm was purged with filtered air every two weeks (Fig. 4). Microcosms were removed from the incubator and after peeling back the aluminum cap, the rubber stopper was sterilized with 70% ethanol. Syringe filters with a pore size of 0.22  $\mu\text{m}$  were applied to the end of a tube connected to a pressurized air line, and the filters were then fitted with a 25-27 G needle; this needle was inserted into the middle of the rubber stopper. A second needle, not connected to any filter or air line, was also inserted into each rubber stopper to prevent the pressurization of the microcosms. Each microcosm was purged with sterile air for two minutes, and needles were changed between treatments. Due to the accumulation of needle holes, the rubber stoppers were replaced in the 12-week and 20-week microcosms at the 8-week timepoint to maintain an airtight seal.

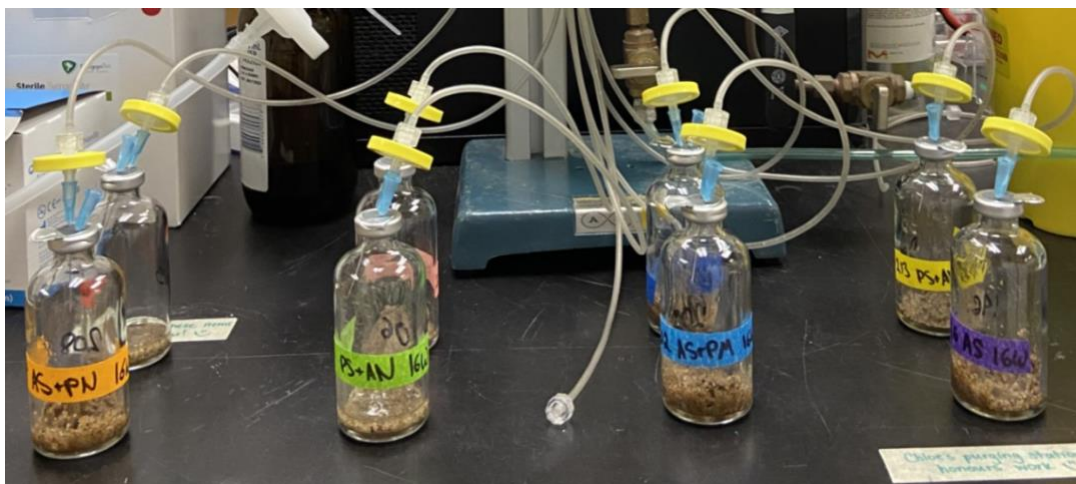


Figure 4. Manifold setup used to purge eight microcosms at a time.

## 2.3 Sampling of microcosms

### 2.3.1 DNA extraction

DNA was extracted from a 0.5 g subsample of soil from each microcosm using the PowerSoil Pro DNA Extraction Kit (Qiagen, Hilden, Germany). The extraction was performed according to the manufacturer's protocol with one exception: a FastPrep-24™ (Fisher Scientific, Hampton, United States) was used to perform the bead beating at 6.0 m/s for two intervals of 60 seconds with a five-minute rest period.

### 2.3.2 Library preparation

The V3 and V4 regions of the 16S ribosomal RNA gene were targeted in polymerase chain reaction (PCR) using primer set 341F (5'- TACGGGAGGCAGCAG - 3') and 806R (5'- GGACTACVSGGGTATCTAAT - 3') to reveal the microbial community compositions within each microcosm. Each individual 20 µl PCR was composed of 10 µl of G2 GoTaq (Promega, USA), 4 µl PCR-quality water, 0.5 µM of forward primer, 0.5 µM of reverse primer, and 4 µl of DNA template. Thermocycling conditions for the first round of amplification were set as 95.0°C for 4 minutes (initial denaturation), followed by 30 cycles of denaturation at 95.0°C for 30 seconds, annealing at 53.4°C for 45 seconds, extension at 72°C for 2 minutes, and a final extension at 72°C

for 5 minutes. Negative controls, in which sterile water was included instead of template DNA, were included with each set of reactions to verify that there was no contamination.

The quality of the amplicons produced was confirmed using gel electrophoresis; a 100 ml 1.0 % agarose gel was made using 1X TAE buffer (40 mM Tris, 20 mM Acetate, and 1mM EDTA) and 5µl of 20,000X RedSafe™ Nucleic Acid Staining Solution (FroggaBio, Toronto, Canada). Samples were loaded into the wells and a constant voltage of 80V was applied for 45 minutes in 1X TAE buffer at room temperature. Gels contained 500 ng of a 100 bp DNA ladder (FroggaBio, Toronto, Canada) as a size marker. The amplicons were then purified using AMPure XP bead-based reagent (Beckman Coulter, Brea, USA) to remove free primers and primer dimer, salts, enzymes, and other remaining PCR reagents.

Following purification, a second round of PCR amplification was performed with adaptor and Ion Xpress barcoded primers [341F (5'-CCATCTCATCCCTGCGTGTCTCCGACTCAG[barcode]TACGGGAGGCAGCAG-3'); 806R (5'-CCACTACGCCTCCGCTTTCCTCTCTATGGGCAGTCGGTGATGGACTACVSGGGTATCTAAT-3')]. The second round of 20 µl reactions included 10 µl of G2 GoTaq, 5 µl PCR-quality water, 0.5 µM of forward primer, 0.5 µM of reverse primer, and 3 µl of DNA template; cycling conditions for this second round of PCR were set as 95.0°C for 4 minutes (initial denaturation), followed with 25 cycles of denaturation at 95.0°C for 30 seconds, annealing at 65.0°C for 45 seconds, extension at 72°C for 2 minutes, and a final extension at 72°C for 5 minutes. After the second round of amplification was complete, the amplicons were purified using AMPure XP bead-based reagent and the purified product was quantified using the Qubit™ dsDNA High Sensitivity kit (Thermo Fisher Scientific, Waltham, USA). Based on the measured concentrations, samples were pooled and purified again using a MicroElute Gel Extraction Kit (Omega Bio-Tek, Norcross, USA) according to the manufacturers protocol.

### *2.3.3 16S rRNA gene sequencing and data processing*

Concentrations of pooled PCR products were determined by qPCR using an Ion Library TaqMan™ Quantification Kit on a QuantStudio 3 qPCR instrument (Applied Bioscience, Waltham,

USA). The pooled libraries were then diluted to equimolar amounts and prepared for sequencing using an Ion 510 & Ion 520 & Ion 530 Chef Reagents kit and Ion 530 chips on the Ion Chef system. Sequencing was done using the Ion Torrent S5 XL system with 400 base pair chemistry (Thermo Fisher Scientific, Waltham, USA). Basecalling was done in Torrent Suite 5.18.1 and data were exported in fastq format prior to demultiplexing in AMPtk 1.5.5 (Palmer et al., 2018) using the `amptk ion` script with default settings except that `--trim-len` was set to 350 bases. Demultiplexed data were imported into Qiime 2 (2023.9.2; `q2cli` 2023.9.1) with the `qiime tools import` script set with `--input-format SingleEndFastqManifestPhred33V2` (Bolyen et al., 2019). Denoising was done with `qiime2 dada2 denoise-single` with `max-ee` set to 1.0 (`p-trunc-len` was set to 0 as the reads were already trimmed in AMPtk). The `qiime feature-classifier classify-sklearn` script was used to assign taxonomy with a Greengenes2 (2022.10) database (McDonald et al., 2023) trained in `qiime2` using `q2-feature-classifier` with the 341f-806r primers used for this study. Of the total 226 samples sequenced, 220 samples met the minimum read requirement of >10,000 reads, and a total of 1742 amplicon sequence variants (ASVs) were observed.

#### 2.4 Data analysis

Phylum-level bar plots were generated by converting the number of reads to the proportion of reads observed in each sample by dividing the number of reads for each phylum by the total number of reads for the sample. Statistical analyses were completed in RStudio using the *vegan* package (Oksanen et al., 2022). Read counts were rarified to an even depth of 11,026 reads using the *phyloseq* package in RStudio to achieve equal sampling depth across samples, and the rarified ASV table was used for all downstream analyses. Beta diversity was investigated to examine differences in community composition between treatments and between time points; beta diversity was examined by calculating the Bray-Curtis dissimilarity of the log transformed ASV data and these values were visualized using multidimensional scaling plots (MDS) created in RStudio using the packages *vegan* and *ggplot*.

To assess the statistical significance of the differences in microbial community compositions between sample groups, the `adonis` function in the *vegan* package was used to conduct Permutational Multivariate Analysis of Variance (PERMANOVA). If two communities were found to be significantly different from each other, a Similarity Percentage (SIMPER) test

was performed to determine how much of the dissimilarity between the communities could be explained by differences in abundance of individual ASVs between sample groups.

### 3. RESULTS

#### *3.1 Characterizing microbial community composition at two field sites in the Canadian High Arctic*

The Time 0 microcosms were examined to compare the initial microbial community composition of the permafrost and active layer within the Long Point and Augustus Hills field sites, as well as to compare each layer between sites. The control treatment (PS or AS) was grouped with the nutrient treatment (PS+AN or AS+PN) for both the permafrost and active layer since both treatments do not include the addition of microbes from the opposite layer. Therefore, sequencing of the 16S rRNA gene amplicons revealed the microbial community composition within six permafrost microcosms and six active layer microcosms for each field site (Fig. 5). Sequences were grouped to a total of 63 phyla, with 58 of the phyla being bacterial, and five being archaeal. Of the 63 phyla detected, 48 of these phyla each represented less than 1% of the microbial community in every sample, and these phyla were grouped into the “other” category (Table A.1). The greatest proportion of a microbial community that these grouped phyla made up was 1.61%. The remaining 15 phyla included 14 bacterial phyla, and 1 archaeal phylum (Thermoproteota).

At Time 0, the Long Point microcosms (Fig. 5A) were dominated by Actinobacteriota, Proteobacteria, and Acidobacteriota at the phylum level; three of the permafrost-dominant samples were also dominated by Firmicutes\_D, which was less abundant in the active layer-dominant samples. Like the Long Point microcosms, at Time 0 the Augustus Hills microcosms (Fig. 5B) also were dominated by Actinobacteriota, Proteobacteria and Acidobacteriota, with Firmicutes\_D being more abundant in all six permafrost-dominant samples than in the active layer-dominant samples.

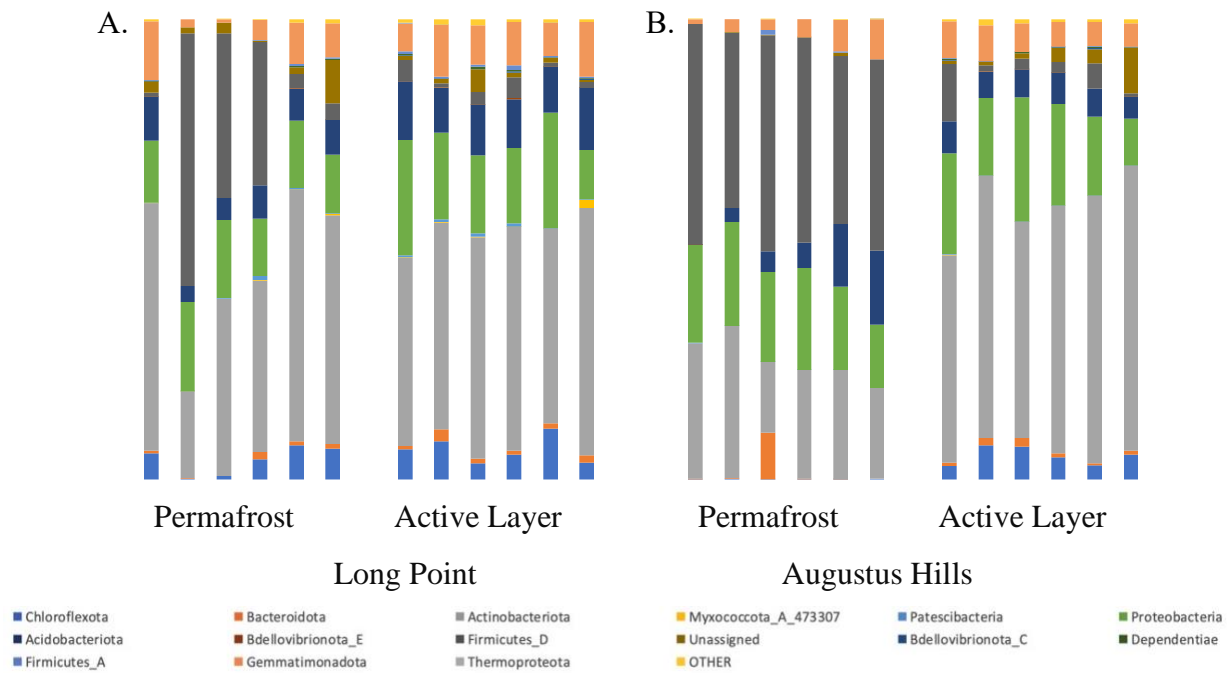


Figure 5. Relative abundances of phyla observed in the permafrost and active layer microcosms at Time 0 for both field sites. The “OTHER” category represents grouped phyla that each made up less than 1% of every sample.

An MDS plot was created to visualize the Bray-Curtis dissimilarity between the permafrost and active layer microbial community compositions for both field sites at Time 0 (Fig. 6). The Long Point samples grouped separately from the Augustus Hills samples for both the permafrost and active layer; using PERMANOVA tests to compare field sites revealed that both the active layer community composition ( $\text{Pr}(>F) = 0.004$ ) and the permafrost community composition ( $\text{Pr}(>F) = 0.011$ ) were significantly different between the two field sites. A SIMPER test revealed that the cumulative contributions of three ASVs were responsible for 27.0% of the variation between the Long Point and Augustus Hills permafrost community compositions (Table A.2); these three ASVs included members of the Firmicutes, Proteobacteria, and Actinobacteriota phyla. The largest contribution to the difference in permafrost community composition between the Long Point and Augustus Hills samples was attributed to *Caldalkalibacillus thermarum*, a member of the Firmicutes phylum, which explained 15.8% of the difference in community composition and was more abundant in the Augustus Hills permafrost samples than in the Long Point permafrost samples.

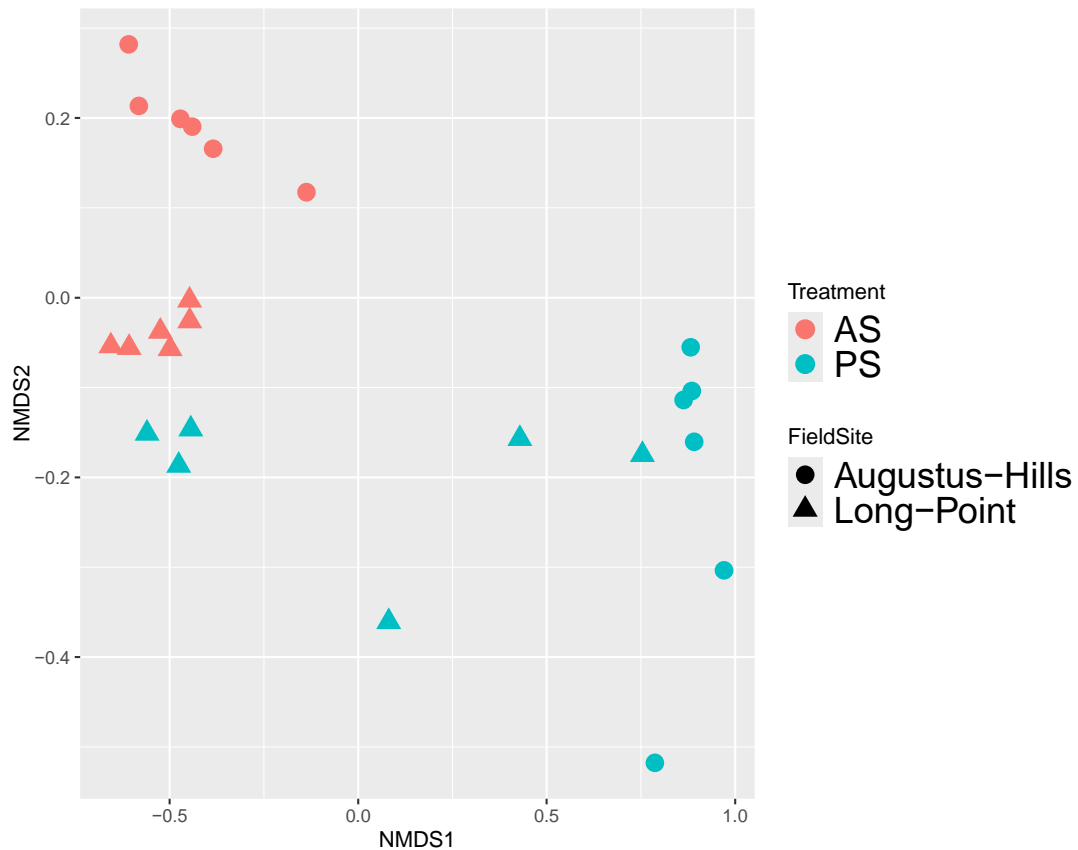


Figure 6. MDS Plot representing the Bray-Curtis dissimilarity in microbial community composition between the microcosms containing active layer or permafrost soil at Time 0 for both the Long Point and Augustus Hills field sites.

For the Long Point and Augustus Hills active layer community compositions, 28.0% of the difference between communities could be explained by three ASVs, which included two members of the Actinobacteriota phylum, and one member of the Proteobacteria phylum (Table A.3). The greatest contributor to the difference between the active layer communities of the two field sites was a member of the Actinobacteriota phylum in the family Micrococcaceae, which explained 10.6% of the difference between communities and was more abundant in the Augustus Hills active layer samples than in the Long Point active layer samples.

The permafrost and active layer microbial community compositions were compared within each field site; Figure 6 shows that the active layer and permafrost samples group separately from each other for both field sites. The Long Point permafrost and active layer samples were found to

be statistically different from one another ( $\text{Pr}( > F ) = 0.008$ ). The three ASVs with the largest influence on the dissimilarity of microbial community compositions were members of the Firmicutes, Actinobacteriota, and Proteobacteria phyla, which cumulatively explained 22.2% of the difference in community composition (Table A.4). The member of the Firmicutes phyla, *Caldalkalibacillus thermarum*, had the greatest contribution to the difference between the Long Point permafrost and active layer communities, explaining 11.8% of the difference. *Caldalkalibacillus thermarum* was found to be more abundant in the permafrost samples than in the active layer samples.

The Augustus Hills permafrost and active layer samples showed distinct groupings on the MDS plot, and the microbial community compositions were found to be significantly different from each other ( $\text{Pr}( > F ) = 0.001$ ). One member of the Firmicutes phylum and two members of the Actinobacteriota phylum cumulatively explained 29.6% of the difference between the Augustus Hills active layer and permafrost samples (Table A.5). Again, *Caldalkalibacillus thermarum* had the greatest contribution to the difference between communities, explaining 16.0% of the difference and being more abundant in the permafrost samples than in the active layer samples.

### 3.2 The effect of permafrost thaw on microbial community composition

Within each treatment, comparisons of the microbial community composition showed shifts over time in the relative abundances of phyla (Fig. 7). The dominant phyla observed in the Long Point microcosms remained the same following thaw: Actinobacteriota, Proteobacteria, and Acidobacteriota dominated all treatments, with Firmicutes\_D being more abundant in the permafrost-dominant samples than in the active layer-dominant samples. The Augustus Hills microcosms underwent a greater shift in the relative abundances of phyla than the Long Point microcosms, especially in the permafrost-dominant treatments. The active layer-dominant samples maintained the same three dominant phyla (Actinobacteriota, Proteobacteria and Acidobacteriota), however in the AS+PM and the AS+PM+PN treatments, Firmicutes\_D also became a dominant phylum following thaw. The most abundant phyla in the permafrost-dominant Augustus Hills treatments changed in response to thaw: the relative abundance of Proteobacteria and Actinobacteriota decreased while the relative abundance of Acidobacteriota increased. The Gemmatimonadota phylum also underwent an increase in relative abundance in the Augustus Hills

permafrost-dominant microcosms following thaw. Therefore, the dominant phylum in the permafrost-dominant treatments shifted following thaw to include the Gemmatimonadota, Acidobacteriota and Firmicutes\_D phyla in all four permafrost-dominant treatments.

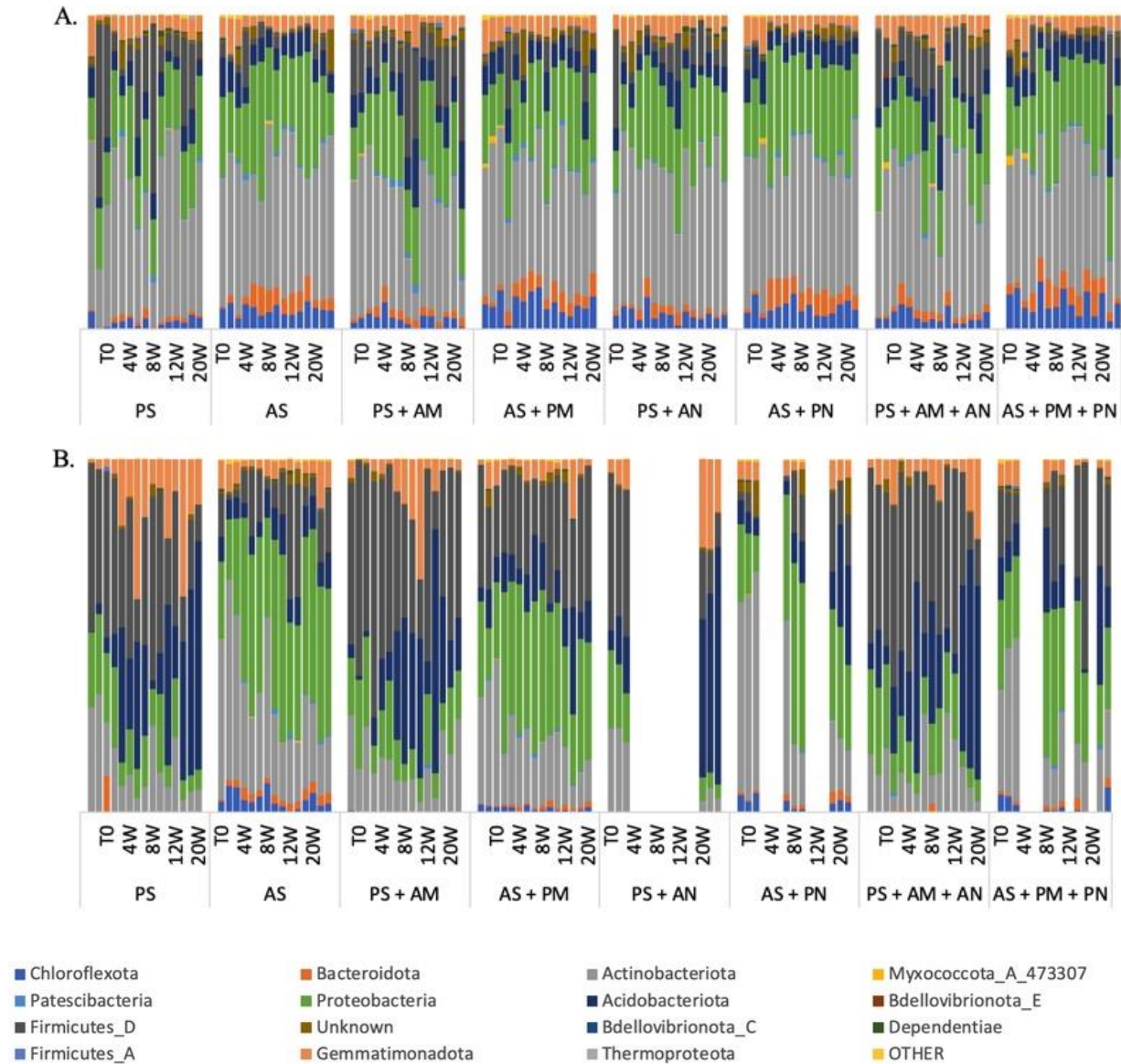


Figure 7. Relative abundances of phyla observed in the Long Point (A) and Augustus Hills (B) experimental microcosms. The “OTHER” category represents grouped phyla that each made up less than 1% of every sample. Missing samples were either not created due to complications in experiment set up or were removed from analysis due to having fewer than 10,000 reads.

### *3.2.1 The influence of microbial dispersal and nutrient inputs on the post-thaw microbial community composition of the Long Point samples*

Due to the Long Point permafrost and active layer soil containing microbial communities that differ from each other as well as from the Augustus Hills samples, the field sites were investigated independently to examine the influence of microbial dispersal, nutrient inputs, and the changing selective pressures associated with thaw on post-thaw microbial community composition. MDS plots were created to visualize the Bray-Curtis dissimilarity in community composition between samples. The active layer-dominant and permafrost-dominant treatments grouped separately from each other on the MDS plot (Fig. 8A). Comparing timepoints, the treatment effect appears to be resolved by the 4-week timepoint.

Looking at only the active layer-dominant treatments, the MDS plot reveals that the initial community composition (Time 0) was similar across treatments (Fig. 8B). There is a clear shift from the initial microbial community composition to the post-thaw microbial community composition across all treatments. This shift was confirmed using a PERMANOVA test to compare the initial and post-thaw community compositions within treatments, followed by using a SIMPER test to determine the community members with the largest contributions to the community composition change.

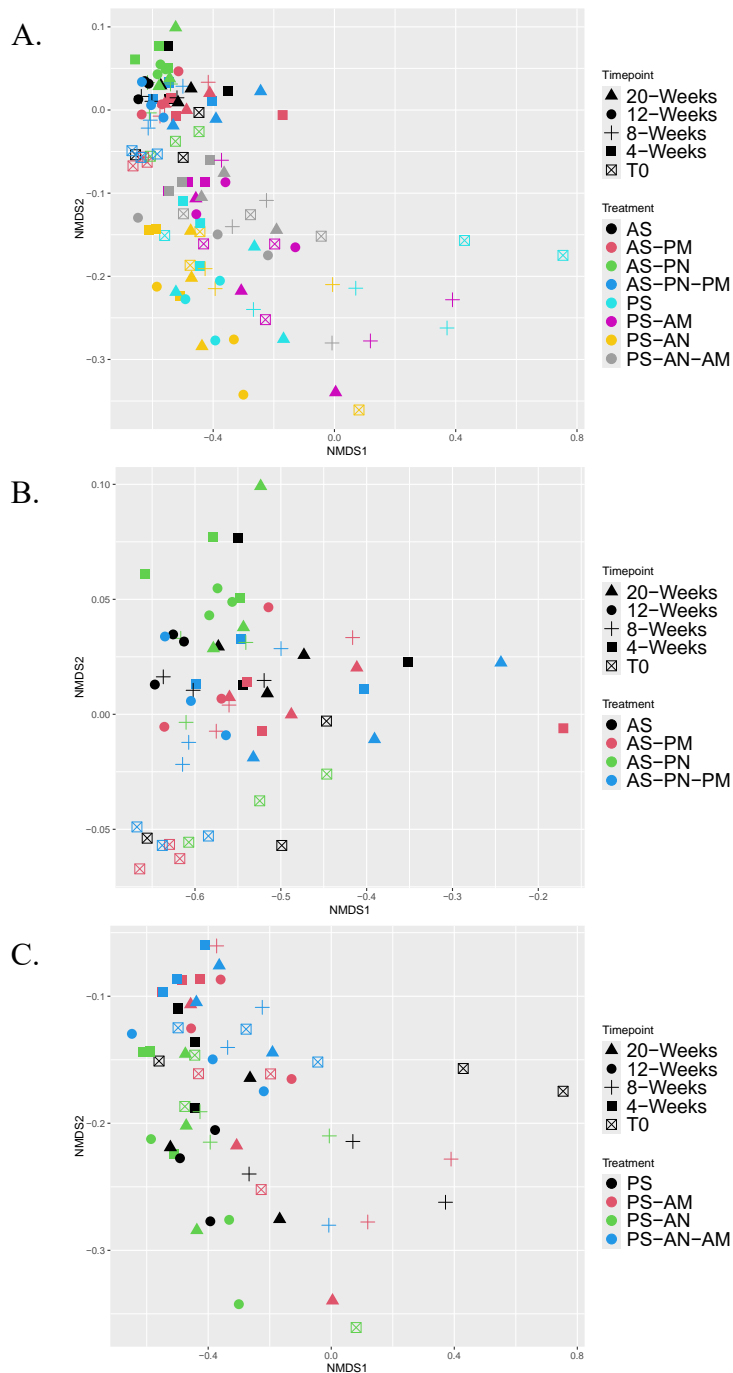


Figure 8. MDS Plots representing the Bray-Curtis dissimilarity in microbial community composition between (A) all Long Point treatments microcosms, (B) active layer-dominant Long Point microcosms, and (C) permafrost-dominant Long Point microcosms.

The AS treatment community composition significantly changed following thaw ( $\text{Pr}( > F ) = 0.002$ ); a total of 23.8% of the difference could be explained by the top three contributors to the change in community composition (Table A.6). These community members included one member

of the Proteobacteria phylum, and two members of the Actinobacteriota phylum. The AS+PM treatment samples also changed significantly following thaw ( $\text{Pr}( > F ) = 0.005$ ). 19.4% of the variation between communities could be explained by the three community members with the greatest contributions to the difference in community composition following thaw: one member of the Proteobacteria phylum, one member of the Actinobacteriota phylum, and one member of an unidentified bacterial phylum (Table A.7). The AS+PN treatment samples showed a significant change in community composition post-thaw ( $\text{Pr}( > F ) = 0.006$ ), with one member of the Proteobacteria phylum and two members of the Actinobacteriota phylum cumulatively explaining 24.7% of the difference in community composition (Table A.8). Curiously, it was the same unassigned member of the Proteobacteria phylum that had the greatest contribution to the difference between initial and post-thaw communities for the AS, AS+PM, and the AS+PN treatments. Lastly, the AS+PM+PN treatment also changed over time in response to thaw ( $\text{Pr}( > F ) = 0.006$ ). The three community members that had the largest contributions to the difference in community composition collectively explained 13.4% of the difference and included two members of the Actinobacteriota phylum and one member of the phylum Firmicutes (Table A.9).

In terms of the permafrost-dominant treatments, the initial and post-thaw community composition varied between treatments, and the shift between initial and post-thaw community composition was not consistent across treatments (Fig.8C). The MDS plot does not reveal any consistent shifts in microbial community composition following thaw. Two of the Long Point permafrost-dominant treatments did not show a significant change in microbial community composition in response to thaw: PS and PS+AN. Interestingly, both treatments that included the addition of active layer microorganisms (PS+AM and PS+AM+AN) showed significant change in community composition following thaw ( $\text{Pr}( > F ) = 0.044$  and  $\text{Pr}( > F ) = 0.001$ , respectively). For the PS+AM treatment samples, 19.0% of the variation between communities could be explained by the three community members that had the greatest contributions to the difference between initial and post-thaw communities: members of the Firmicutes, Actinobacteriota, and the Proteobacteria phyla (Table A.10). For the PS+AM+AN treatment samples, the three community members that had the greatest contributions to the difference between initial and post-thaw communities also included members of the Firmicutes, Actinobacteriota, and Proteobacteria phyla, which

cumulatively explained 22.0% of the variation between microbial community compositions (Table A.11).

### *3.2.2 The influence of microbial dispersal and nutrient inputs on the post-thaw microbial community composition of the Augustus Hills samples.*

To examine the influence of microbial dispersal, nutrient inputs, and the changing selective pressures associated with permafrost thaw on post-thaw microbial community composition in the Augustus Hills microcosms, MDS plots were created to visualize the Bray-Curtis dissimilarity in community composition between samples. The Augustus Hills active layer-dominant and permafrost-dominant treatments grouped separately from each other on the MDS plot, and the treatment effect appears to be resolved by the 8-week timepoint. (Figure 9A).

The initial community composition of the Augustus Hills active layer-dominant samples varied between treatments (Fig. 9B). However, thaw influenced the microbial community composition in similar ways across all treatments. The AS+PN treatment samples group very closely to the AS treatment samples both pre- and post-thaw; this indicates that the addition of permafrost nutrients to active layer soil does not drive changes in community composition that differ from the changes observed in the active layer soil without the addition of nutrients post-thaw. The treatments that include the addition of permafrost microbes (AS+PM and AS+PM+PN) are distinct from the treatments that do not include the addition of permafrost microbes (AS and AS+PN) both initially and following thaw.

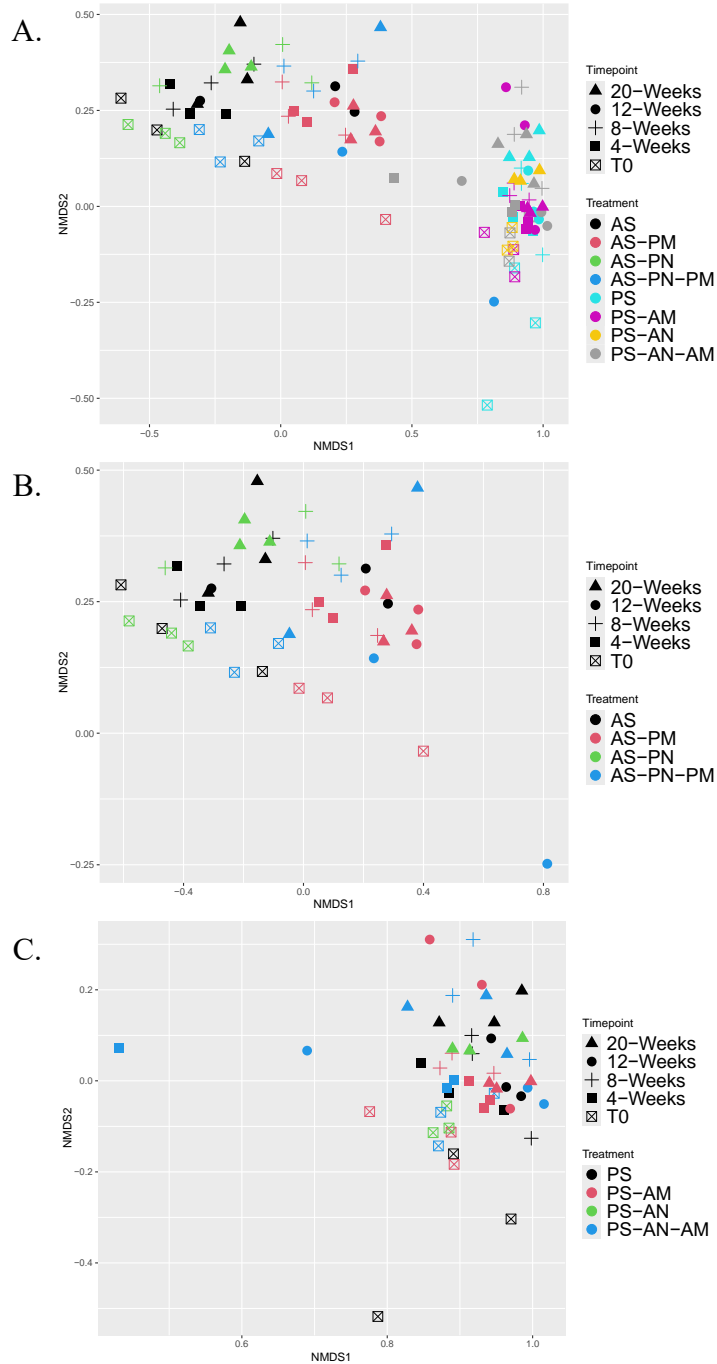


Figure 9. MDS Plots representing the Bray-Curtis dissimilarity in microbial community composition between (A) all Augustus Hills treatments microcosms, (B) active layer-dominant Augustus Hills microcosms, and (C) permafrost-dominant Augustus Hills microcosms.

The shift in the microbial community composition of the AS treatment samples following thaw was significant ( $\text{Pr}(>F) = 0.002$ ), and the ASVs with the greatest contributions to the change in community composition were found to be members of the Actinobacteriota, Firmicutes, and

Proteobacteria phyla which cumulatively explained 27.1% of the difference (Table A.12). The change in microbial community composition post-thaw was also significant for the AS+PN treatment ( $\text{Pr}( > F ) = 0.014$ ); the top three contributors to the dissimilarity in community composition explained 24.7% of the variation and included members of the Actinobacteriota, Acidobacteriota and Firmicutes phyla (Table A.13). Interestingly, the same member of the Actinobacteriota phylum, within the family Micrococcaceae, was the top contributor to the difference in community composition post-thaw for both the AS and AS+PN treatments. For both the dispersal treatments, AS+PM and AS+PM+PN, microbial community composition changed significantly following thaw ( $\text{Pr}( > F ) = 0.004$  and  $\text{Pr}( > F ) = 0.006$ , respectively). The top three ASVs with the greatest contributions to the changes in microbial community composition were identical between the AS+PM and AS+PM+PN treatments; these three ASVs included one member of the Firmicutes phylum and two members of the Actinobacteriota phylum which cumulatively explained 24.7% of the dissimilarity in the AS+PM treatment microcosms (Table A.14), and 24.6% of the dissimilarity in the AS+PM+PN treatment microcosms (Table A.15). It is notable that the largest contributor to the variation observed in these two treatments was *Caldalkalibacillus thermanum*, a member of the Firmicutes\_D phylum.

For the Augustus Hills permafrost-dominant samples, the MDS plot revealed that the initial community composition was similar across treatments (Fig. 9). The selective pressures induced by thaw had a similar effect across all the permafrost-dominant treatments. All four active-layer dominant treatments showed a significant change in microbial community composition following thaw (PS:  $\text{Pr}( > F ) = 0.006$ ; PS+AM:  $\text{Pr}( > F ) = 0.019$ ; PS+AN:  $\text{Pr}( > F ) = 0.01$ ; PS+AM+AN:  $\text{Pr}( > F ) = 0.02$ ). The PS, PS+AN, and the PS+AM+AN treatments all shared the same three ASVs with the greatest contributions to the change in microbial community composition. These three ASVs were members of the Acidobacteriota, Firmicutes, and Gemmatimonadota phyla, and they cumulatively contributed to 54.0% of the difference in the PS treatment, 61.5% of the difference in the PS+AN treatment, and 50.7% of the difference in the PS+AM+AN treatment (Table A.16, Table A.17, and Table A.18, respectively). The PS+AM treatments differed slightly from the other three treatments in the ASVs with the largest contributions to dissimilarity between communities: the members of the Acidobacteriota and Firmicutes phyla were the same, but the third ASV was a member of the Actinobacteriota phylum. These three ASVs cumulatively explained 47.5% of the difference in

microbial community composition in the PS+AM microcosms following thaw (Table A.19). In all four of the Augustus Hills permafrost-dominant treatments, a member of the Acidobacteriota phylum in the order Vicinamibacteria had the largest contribution to the dissimilarity between community composition.

## 4. DISCUSSION

### *4.1 Characterizing microbial community composition at two field sites in the Canadian High Arctic*

Sequencing of the V3-V4 region of the 16S rRNA gene revealed that the initial microbial community composition within the permafrost and active layer differed between the Long Point and Augustus Hills field sites. This supports the hypothesis that the pre-thaw microbial community composition is different between field sites. The two field sites were dominated by the same phyla: Actinobacteriota, Proteobacteria, and Acidobacteriota were the dominant phyla in both the active layer and permafrost, with Firmicutes\_D also being a dominant phylum in the permafrost samples at both field sites. These dominant phyla are largely in agreement with previous studies examining microbial community compositions in the Arctic (Steven et al., 2007; Steven et al., 2008; Yergeau et al., 2010; Tuoroto et al., 2014; Waldrop et al., 2023). Additionally, the higher abundance of Firmicutes in the permafrost relative to the active layer has been observed in previous studies (Yergeau et al., 2010; Monteux et al., 2018). The results of the present study are also in line with the findings of Hultman et al. (2015), who found that Actinobacteriota, Acidobacteriota and Proteobacteria were the most active phyla in the active layer based on analysis of metatranscriptome measurements, while Proteobacteria, Acidobacteriota, and Firmicutes were the most active phyla in the permafrost. Given that the Long Point and Augustus Hills sites are distinct from each other geographically and that visually the soils appeared very different, there is the assumption that the physicochemical characteristics of the soil differ between these two sites, which likely contributes to the differences observed in microbial community composition. The physicochemical characteristics of the soil at these two sites need to be characterized to relate initial microbial community composition with physicochemical properties of the environment.

Within each field site, the initial active layer microbial community composition was found to be significantly different from the initial permafrost microbial community composition. This result supports the hypothesis that the initial microbial communities in the active layer and permafrost are significantly different from each other at each field site. The active layer and permafrost treatments grouped separately on the MDS plot, as has been observed in previous studies (e.g., Müller et al., 2018; Varsadiya et al., 2021). The Augustus Hills active layer and permafrost sample groups are more distinct from each other on the MDS plot than the Long Point active layer and permafrost sample groups; this suggests that there is greater variation in the pre-thaw microbial community composition between the Augustus Hills active layer and permafrost samples than between the Long Point active layer and permafrost samples. Visually, there appeared to be a greater distinction between the Augustus Hills active layer and permafrost soils than between the Long Point active layer and permafrost soils; this suggests that there is greater variation in physicochemical properties between the Augustus Hills active layer and permafrost than between the Long Point active layer and permafrost, which may influence microbial community composition. The physicochemical properties of both soil types need to be characterized at each field site.

#### *4.2 The effect of permafrost thaw on microbial community composition*

The relative abundances of phyla shifted over time following thaw. The dominant phyla found in the Long Point microcosms remained the same following thaw, whereas the dominant phyla found in the Augustus Hills microcosms shifted. There was also a greater shift in the relative abundances of the phyla found in the Augustus Hills microcosms than in the Long Point microcosms. Since the two field sites had significantly different initial microbial community compositions, the effects of each treatment on the post-thaw microbial community composition were examined at each site individually. The MDS plot revealed that the permafrost- and active layer-dominant samples grouped separately from each other for both field sites pre- and post- thaw.

##### *4.2.1 The influence of microbial dispersal and nutrient inputs on the post-thaw microbial community composition of the Long Point samples*

In the Long Point samples, the treatment effect appears to be resolved early in the experiment with the greatest shifts occurring before the 4-week time point. All four of the active layer-dominant treatments changed significantly following thaw. There is a clear shift from the initial microbial community composition to the post-thaw microbial community composition that is similar across the active layer-dominant treatments. This indicates that the selective pressures associated with the simulated thaw conditions influenced microbial community composition of the active layer-dominant treatments in similar ways. The results of the active layer-dominant treatments do not provide any indication that the permafrost microbes outcompete the active layer microbes following thaw. Therefore, these results provide support for the hypothesis that microbial dispersal from the permafrost to the active layer will not induce stronger shifts in community composition than the changing selective pressures that accompany thaw.

Compared to the active layer-dominant treatments, the Long Point permafrost-dominant treatment samples had more heterogeneity in pre-thaw and post-thaw microbial community compositions. There was no predictable shift across all Long Point permafrost-dominant treatments. Only the treatments that included the dispersal of microbes from the active layer (PS+AM and PS+AM+AN) underwent a significant change in microbial community composition following thaw. The results of the Long Point permafrost-dominant samples provide support for the hypothesis that microbial dispersal from the active layer to the permafrost will have a stronger influence on post-thaw microbial community composition than the changing selective pressures that accompany thaw.

#### *4.2.2 The influence of microbial dispersal and nutrient inputs on the post-thaw microbial community composition of the Augustus Hills samples.*

In the Augustus Hills samples, the treatment effect appears to be resolved by the 8-week timepoint. The initial active layer-dominant treatment samples showed varying microbial community compositions; the treatments that included the addition of the permafrost microbes were more similar initially than the treatments that did not include the addition of permafrost microbes. This pattern continued in the post-thaw samples, which suggests that the influence of the permafrost microbes persists following thaw. All four of the Augustus Hills active layer-dominant treatments underwent significant shifts in microbial community composition following thaw. The

consistent community shifts in the active-layer dominant treatments suggests that the selective pressures associated with thaw were the most important influence in determining post-thaw microbial community composition. Like for the Long Point active layer-dominant treatments, the Augustus Hills active layer-dominant treatments did not provide any evidence that the permafrost microbes outcompete the active layer microbes. Thus, these results support the hypothesis that microbial dispersal from the permafrost to the active layer will not induce stronger shifts in community composition than the changing selective pressures that accompany thaw.

The Augustus Hills initial permafrost-dominant treatment samples showed similar microbial community compositions. All four of the permafrost-dominant treatments changed significantly following thaw and there was a consistent shift observed across treatments. This suggests that the selective pressures induced by thaw influenced all the active layer-dominant treatments in a similar way. The results of the Augustus Hills permafrost-dominant samples do not support the hypothesis that microbial dispersal from the active layer to the permafrost will have a stronger influence on post-thaw microbial community composition than the changing selective pressures that accompany thaw.

#### *4.3 Conclusions*

This study is the first to examine the effects of thaw on the microbial community composition at multiple field sites in the Canadian High Arctic by determining the influence of microbial dispersal and nutrient input. The five-month incubation experiment carried out in this study represents multiple summer cycles in which increased surface temperatures lead to permafrost thaw, making the results of this study important for understanding how microbial communities will change over multiple seasons following permafrost thaw.

The results of this study suggest that the change in selective pressures that accompany thaw (e.g., increase in temperature, nutrient mixing) are the most important ecological factors that influence post-thaw microbial community composition, and that initial microbial community composition is an important factor in determining post-thaw microbial community composition. Together, the results of this study indicate that 1) permafrost microbial communities differ across Arctic landscapes, and 2) microbial community responses to thaw will differ across locations in

the Canadian High Arctic. As such, extrapolating results from the limited range of sites studied across the Arctic to date, and predicting future responses based on this data, is highly problematic given the heterogeneity observed in structure and thaw response in even a small number of samples. Efforts to predict ecological responses to permafrost thaw across Arctic environments will need to be greatly expanded to understand responses to permafrost thaw across the Canadian Arctic.

## 5. LITERATURE CITED

- Adamczyk, M., Rüthi, J., and Frey, B. 2021. Root exudates increase soil respiration and alter microbial community structure in alpine permafrost and active layer soils. *Environmental Microbiology* **23**(4): 2152–2168. doi:[10.1111/1462-2920.15383](https://doi.org/10.1111/1462-2920.15383).
- Allan, J., Ronholm, J., Mykytczuk, N.C.S., Greer, C.W., Onstott, T.C., and Whyte, L.G. 2014. Methanogen community composition and rates of methane consumption in Canadian High Arctic permafrost soils. *Environmental Microbiology Reports* **6**(2): 136–144. John Wiley & Sons, Ltd. doi:[10.1111/1758-2229.12139](https://doi.org/10.1111/1758-2229.12139).
- Bockheim, J.G. 2007. Importance of Cryoturbation in Redistributing Organic Carbon in Permafrost-Affected Soils. *Soil Science Society of America Journal* **71**(4): 1335–1342. doi:[10.2136/sssaj2006.0414N](https://doi.org/10.2136/sssaj2006.0414N).
- Bolyen E, Rideout JR, Dillon MR, Bokulich NA, Abnet CC, Al-Ghalith GA, Alexander H, Alm EJ, Arumugam M, Asnicar F, Bai Y, Bisanz JE, Bittinger K, Brejnrod A, Brislawn CJ, Brown CT, Callahan BJ, Caraballo-Rodríguez AM, Chase J, Cope EK, Da Silva R, Diener C, Dorrestein PC, Douglas GM, Durall DM, Duvallet C, Edwardson CF, Ernst M, Estaki M, Fouquier J, Gauglitz JM, Gibbons SM, Gibson DL, Gonzalez A, Gorlick K, Guo J, Hillmann B, Holmes S, Holste H, Huttenhower C, Huttley GA, Janssen S, Jarmusch AK, Jiang L, Kaehler BD, Kang KB, Keefe CR, Keim P, Kelley ST, Knights D, Koester I, Kosciulek T, Kreps J, Langille MGI, Lee J, Ley R, Liu YX, Loftfield E, Lozupone C, Maher M, Marotz C, Martin BD, McDonald D, McIver LJ, Melnik AV, Metcalf JL, Morgan SC, Morton JT, Naimey AT, Navas-Molina JA, Nothias LF, Orchanian SB, Pearson T, Peoples SL, Petras D, Preuss ML, Pruesse E, Rasmussen LB, Rivers A, Robeson MS, Rosenthal P, Segata N, Shaffer M, Shiffer A, Sinha R, Song SJ, Spear JR, Swafford AD, Thompson LR, Torres PJ, Trinh P, Tripathi A, Turnbaugh PJ, Ul-Hasan S, van der Hooft JJJ, Vargas F, Vázquez-Baeza Y, Vogtmann E, von Hippel M, Walters W, Wan Y, Wang M, Warren J, Weber KC, Williamson CHD, Willis AD, Xu ZZ, Zaneveld JR, Zhang Y, Zhu Q, Knight R, and Caporaso JG. 2019. Reproducible, interactive, scalable and extensible microbiome data science using QIIME 2. *Nature Biotechnology* **37**: 852–857. <https://doi.org/10.1038/s41587-019-0209-9>.
- Bottos, E.M., Kennedy, D.W., Romero, E.B., Fansler, S.J., Brown, J.M., Bramer, L.M., Chu, R.K., Tfaily, M.M., Jansson, J.K., and Stegen, J.C. 2018. Dispersal limitation and thermodynamic constraints govern spatial structure of permafrost microbial communities. *FEMS Microbiology Ecology* **94**(8): fyy110. doi:[10.1093/femsec/fyy110](https://doi.org/10.1093/femsec/fyy110).
- Chen, L., Liang, J., Qin, S., Liu, L., Fang, K., Xu, Y., Ding, J., Li, F., Luo, Y., and Yang, Y. 2016. Determinants of carbon release from the active layer and permafrost deposits on the Tibetan Plateau. *Nat Commun* **7**(1): 13046. Nature Publishing Group. doi:[10.1038/ncomms13046](https://doi.org/10.1038/ncomms13046).
- D’Amico, S., Collins, T., Marx, J.-C., Feller, G., Gerday, C., and Gerday, C. 2006. Psychrophilic microorganisms: challenges for life. *EMBO reports* **7**(4): 385–389. John Wiley & Sons, Ltd. doi:[10.1038/sj.embor.7400662](https://doi.org/10.1038/sj.embor.7400662).

- Doherty, S.J., Barbato, R.A., Grandy, A.S., Thomas, W.K., Monteux, S., Dorrepaal, E., Johansson, M., and Ernakovich, J.G. 2020. The Transition From Stochastic to Deterministic Bacterial Community Assembly During Permafrost Thaw Succession. *Frontiers in Microbiology* **11**. <https://doi.org/10.3389/fmicb.2020.596589>.
- Ernakovich, J.G., Barbato, R.A., Rich, V.I., Schädel, C., Hewitt, R.E., Doherty, S.J., Whalen, E.D., Abbott, B.W., Barta, J., Biasi, C., Chabot, C.L., Hultman, J., Knoblauch, C., Vetter, M.C.Y.L., Leewis, M.-C., Liebner, S., Mackelprang, R., Onstott, T.C., Richter, A., Schütte, U.M.E., Siljanen, H.M.P., Taş, N., Timling, I., Vishnivetskaya, T.A., Waldrop, M.P., and Winkel, M. 2022. Microbiome assembly in thawing permafrost and its feedbacks to climate. *Global Change Biology* **28**(17): 5007–5026. doi:[10.1111/gcb.16231](https://doi.org/10.1111/gcb.16231).
- Farquharson, L.M., Romanovsky, V.E., Cable, W.L., Walker, D.A., Kokelj, S.V., and Nicolsky, D. 2019. Climate Change Drives Widespread and Rapid Thermokarst Development in Very Cold Permafrost in the Canadian High Arctic. *Geophysical Research Letters* **46**(12): 6681–6689. American Geophysical Union (AGU). doi:[10.1029/2019gl082187](https://doi.org/10.1029/2019gl082187).
- Hultman, J., Waldrop, M.P., Mackelprang, R., David, M.M., McFarland, J., Blazewicz, S.J., Harden, J., Turetsky, M.R., McGuire, A.D., Shah, M.B., VerBerkmoes, N.C., Lee, L.H., Mavrommatis, K., and Jansson, J.K. 2015. Multi-omics of permafrost, active layer and thermokarst bog soil microbiomes. *Nature* **521**(7551): 208–212. Nature Publishing Group. doi:[10.1038/nature14238](https://doi.org/10.1038/nature14238).
- Jansson, J.K., and Taş, N. 2014. The microbial ecology of permafrost. *Nature Reviews Microbiology* **12**(6): 414–425. Springer Nature. doi:[10.1038/nrmicro3262](https://doi.org/10.1038/nrmicro3262).
- Jones A, Stolbovoy V, Tarnocai C, Broll G, Spaargaren O, Montanarella L, Anisimov O, Arnalds Ö, Arnoldussen A, Bockheim J, Breuning-Madsen H, Brown J, Desyatkin R, Goryachkin S, Jakobsen B, Konyushkov D, Mazhitova G, Mccallum I, Naumov E, Overduin P, Nilsson S, Solbakken E, Ping C, Ritz K. Soil Atlas of the Northern Circumpolar Region. EUR 23499 EN. Luxembourg (Luxembourg): Publications Office of the European Union; 2010. JRC47340
- Lawrence, D.M., and Slater, A.G. 2005. A projection of severe near-surface permafrost degradation during the 21st century. *Geophysical Research Letters* **32**(24). doi:[10.1029/2005GL025080](https://doi.org/10.1029/2005GL025080).
- Liang, R., Lau, M., Vishnivetskaya, T., Lloyd, K.G., Wang, W., Wiggins, J., Miller, J., Pfiffner, S., Rivkina, E.M., and Onstott, T.C. 2019. Predominance of Anaerobic, Spore-Forming Bacteria in Metabolically Active Microbial Communities from Ancient Siberian Permafrost. *Appl Environ Microbiol* **85**(15): e00560-19. doi:[10.1128/AEM.00560-19](https://doi.org/10.1128/AEM.00560-19).
- Mackelprang, R., Burkert, A., Haw, M., Mahendrarajah, T., Conaway, C.H., Douglas, T.A., and Waldrop, M.P. 2017. Microbial survival strategies in ancient permafrost: insights from metagenomics. *ISME J* **11**(10): 2305–2318. Nature Publishing Group. doi:[10.1038/ismej.2017.93](https://doi.org/10.1038/ismej.2017.93).

- Mackelprang, R., Saleska, S.R., Jacobsen, C.S., Jansson, J.K., and Taş, N. 2016. Permafrost Metagenomics and Climate Change. *Annu. Rev. Earth Planet. Sci.* **44**(1): 439–462. Annual Reviews. doi:[10.1146/annurev-earth-060614-105126](https://doi.org/10.1146/annurev-earth-060614-105126).
- Mackelprang, R., Waldrop, M.P., DeAngelis, K.M., David, M.M., Chavarria, K.L., Blazewicz, S.J., Rubin, E.M., and Jansson, J.K. 2011. Metagenomic analysis of a permafrost microbial community reveals a rapid response to thaw. *Nature* **480**(7377): 368–371. Nature Publishing Group. doi:[10.1038/nature10576](https://doi.org/10.1038/nature10576).
- McDonald, D., Jiang, Y., Balaban, M., Cantrell, K., Zhu, Q., Gonzalez, A., Morton, J.T., Nicolaou, G., Parks, D.H., Karst, S.M., Albertsen, M., Hugenholtz, P., DeSantis, T., Song, S.J., Bartko, A., Havulinna, A.S., Jousilahti, P., Cheng, S., Inouye, M., Niiranen, T., Jain, M., Salomaa, V., Lahti, L., Mirarab, S., and Knight, R. 2023. Greengenes2 unifies microbial data in a single reference tree. *Nat Biotechnol*: 1–4. Nature Publishing Group. doi:[10.1038/s41587-023-01845-1](https://doi.org/10.1038/s41587-023-01845-1).
- Metcalf, D.B., Hermans, T.D.G., Ahlstrand, J., Becker, M., Berggren, M., Björk, R.G., Björkman, M.P., Blok, D., Chaudhary, N., Chisholm, C., Classen, A.T., Hasselquist, N.J., Jonsson, M., Kristensen, J.A., Kumordzi, B.B., Lee, H., Mayor, J.R., Prev y, J., Pantazatou, K., Rousk, J., Sponseller, R.A., Sundqvist, M.K., Tang, J., Uddling, J., Wallin, G., Zhang, W., Ahlstr m, A., Tenenbaum, D.E., and Abdi, A.M. 2018. Patchy field sampling biases understanding of climate change impacts across the Arctic. *Nat Ecol Evol* **2**(9): 1443–1448. Nature Publishing Group. doi:[10.1038/s41559-018-0612-5](https://doi.org/10.1038/s41559-018-0612-5).
- Monteux, S., Weedon, J.T., Blume-Werry, G., Gavazov, K., Jassey, V.E.J., Johansson, M., Keuper, F., Olid, C., and Dorrepaal, E. 2018. Long-term in situ permafrost thaw effects on bacterial communities and potential aerobic respiration. *ISME J* **12**(9): 2129–2141. Nature Publishing Group. doi:[10.1038/s41396-018-0176-z](https://doi.org/10.1038/s41396-018-0176-z).
- M ller, O., Bang-Andreasen, T., White III, R.A., Elberling, B., Taş, N., Kneafsey, T., Jansson, J.K., and  vre s, L. 2018. Disentangling the complexity of permafrost soil by using high resolution profiling of microbial community composition, key functions and respiration rates. *Environmental Microbiology* **20**(12): 4328–4342. doi:[10.1111/1462-2920.14348](https://doi.org/10.1111/1462-2920.14348).
- Nemergut, D.R., Schmidt, S.K., Fukami, T., O’Neill, S.P., Bilinski, T.M., Stanish, L.F., Knelman, J.E., Darcy, J.L., Lynch, R.C., Wickey, P., and Ferrenberg, S. 2013. Patterns and Processes of Microbial Community Assembly. *Microbiology and Molecular Biology Reviews* **77**(3): 342–356. American Society for Microbiology. doi:[10.1128/mnbr.00051-12](https://doi.org/10.1128/mnbr.00051-12).
- Oksanen, J., Simpson, G.L., Blanchet, F.G., Kindt, R., Legendre, P., Minchin, P.R., O’Hara, R.B., Solymos, P., Stevens, M.H.H., Szoecs, E., Wagner, H., Barbour, M., Bedward, M., Bolker, B., Borcard, D., Carvalho, G., Chirico, M., Caceres, M.D., Durand, S., Evangelista, H.B.A., FitzJohn, R., Friendly, M., Furneaux, B., Hannigan, G., Hill, M.O., Lahti, L., McGlinn, D., Ouellette, M.-H., Cunha, E.R., Smith, T., Stier, A., Braak, C.J.F.T., and Weedon, J. 2022, October 11. vegan: Community Ecology Package. Available from <https://cran.r-project.org/web/packages/vegan/index.html>

- Palmer, J.M., Jusino, M.A., Banik, M.T., and Lindner, D.L. 2018. Non-biological synthetic spike-in controls and the AMPtk software pipeline improve mycobiome data. *PeerJ* **6**: e4925. PeerJ Inc. doi:[10.7717/peerj.4925](https://doi.org/10.7717/peerj.4925).
- Qin, S., Kou, D., Mao, C., Chen, Y., Chen, L., and Yang, Y. 2021. Temperature sensitivity of permafrost carbon release mediated by mineral and microbial properties. *Science Advances* **7**(32): eabe3596. American Association for the Advancement of Science. doi:[10.1126/sciadv.abe3596](https://doi.org/10.1126/sciadv.abe3596).
- Ramage, J., Jungsberg, L., Meyer, A., and Gartler, S. 2022. ‘No longer solid’: perceived impacts of permafrost thaw in three Arctic communities. *Polar Geography* **45**(3): 226–239. Taylor & Francis. doi:[10.1080/1088937X.2022.2105973](https://doi.org/10.1080/1088937X.2022.2105973).
- Rampelotto, P.H. 2014. Polar Microbiology: Recent Advances and Future Perspectives. *Biology (Basel)* **3**(1): 81–84. doi:[10.3390/biology3010081](https://doi.org/10.3390/biology3010081).
- Rantanen, M., Karpechko, A.Y., Lipponen, A., Nordling, K., Hyvärinen, O., Ruosteenoja, K., Vihma, T., and Laaksonen, A. 2022. The Arctic has warmed nearly four times faster than the globe since 1979. *Commun Earth Environ* **3**(1): 1–10. Nature Publishing Group. doi:[10.1038/s43247-022-00498-3](https://doi.org/10.1038/s43247-022-00498-3).
- Saidi-Mehrabad, A., Neuberger, P., Hajihosseini, M., Froese, D., and Lanoil, B.D. 2020. Permafrost Microbial Community Structure Changes Across the Pleistocene-Holocene Boundary. *Frontiers in Environmental Science* **8**. <https://doi.org/10.3389/fenvs.2020.00133>
- Schuur, E. a. G., McGuire, A.D., Schädel, C., Grosse, G., Harden, J.W., Hayes, D.J., Hugelius, G., Koven, C.D., Kuhry, P., Lawrence, D.M., Natali, S.M., Olefeldt, D., Romanovsky, V.E., Schaefer, K., Turetsky, M.R., Treat, C.C., and Vonk, J.E. 2015. Climate change and the permafrost carbon feedback. *Nature* **520**(7546): 171–179. Nature Publishing Group. doi:[10.1038/nature14338](https://doi.org/10.1038/nature14338).
- Schuur, E.A.G., Bockheim, J., Canadell, J.G., Euskirchen, E., Field, C.B., Goryachkin, S.V., Hagemann, S., Kuhry, P., Laflour, P.M., Lee, H., Mazhitova, G., Nelson, F.E., Rinke, A., Romanovsky, V.E., Shiklomanov, N., Tarnocai, C., Venevsky, S., Vogel, J.G., and Zimov, S.A. 2008. Vulnerability of Permafrost Carbon to Climate Change: Implications for the Global Carbon Cycle. *BioScience* **58**(8): 701–714. doi:[10.1641/B580807](https://doi.org/10.1641/B580807).
- Schuur, E.A.G., and Mack, M.C. 2018. Ecological Response to Permafrost Thaw and Consequences for Local and Global Ecosystem Services. *Annu. Rev. Ecol. Evol. Syst.* **49**(1): 279–301. Annual Reviews. doi:[10.1146/annurev-ecolsys-121415-032349](https://doi.org/10.1146/annurev-ecolsys-121415-032349).
- Steven, B., Briggs, G., McKay, C.P., Pollard, W.H., Greer, C.W., and Whyte, L.G. 2007. Characterization of the microbial diversity in a permafrost sample from the Canadian high Arctic using culture-dependent and culture-independent methods: Microbial diversity in Canadian high Arctic permafrost. *FEMS Microbiology Ecology* **59**(2): 513–523. doi:[10.1111/j.1574-6941.2006.00247.x](https://doi.org/10.1111/j.1574-6941.2006.00247.x).

- Steven, B., Pollard, W.H., Greer, C.W., and Whyte, L.G. 2008. Microbial diversity and activity through a permafrost/ground ice core profile from the Canadian high Arctic. *Environmental Microbiology* **10**(12): 3388–3403. John Wiley & Sons, Ltd. doi:[10.1111/j.1462-2920.2008.01746.x](https://doi.org/10.1111/j.1462-2920.2008.01746.x).
- Tarnocai, C., Canadell, J.G., Schuur, E. a. G., Kuhry, P., Mazhitova, G., and Zimov, S. 2009. Soil organic carbon pools in the northern circumpolar permafrost region. *Global Biogeochemical Cycles* **23**(2). doi:[10.1029/2008GB003327](https://doi.org/10.1029/2008GB003327).
- Tuorto, S.J., Darias, P., McGuinness, L.R., Panikov, N., Zhang, T., Haeggbloom, M.M., and Kerkhof, L.J. 2014. Bacterial genome replication at subzero temperatures in permafrost. *ISME J.* **8**(1): 139–149. Nature Publishing Group, London. doi:[10.1038/ismej.2013.140](https://doi.org/10.1038/ismej.2013.140).
- Varsadiya, M., Urich, T., Hugelius, G., and Bárta, J. 2021. Microbiome structure and functional potential in permafrost soils of the Western Canadian Arctic. *FEMS Microbiology Ecology* **97**(3): fiab008. doi:[10.1093/femsec/fiab008](https://doi.org/10.1093/femsec/fiab008).
- Vellend, M. 2010. Conceptual Synthesis in Community Ecology. *The Quarterly Review of Biology* **85**(2): 183–206. The University of Chicago Press. doi:[10.1086/652373](https://doi.org/10.1086/652373).
- Waldrop, M.P., Chabot, C.L., Liebner, S., Holm, S., Snyder, M.W., Dillon, M., Dudgeon, S.R., Douglas, T.A., Leewis, M.-C., Walter Anthony, K.M., McFarland, J.W., Arp, C.D., Bondurant, A.C., Taş, N., and Mackelprang, R. 2023. Permafrost microbial communities and functional genes are structured by latitudinal and soil geochemical gradients. *ISME J* **17**(8): 1224–1235. Nature Publishing Group. doi:[10.1038/s41396-023-01429-6](https://doi.org/10.1038/s41396-023-01429-6).
- Yergeau, E., Hogues, H., Whyte, L.G., and Greer, C.W. 2010. The functional potential of high Arctic permafrost revealed by metagenomic sequencing, qPCR and microarray analyses. *ISME Journal: Multidisciplinary Journal of Microbial Ecology* **4**(9): 1206–1214. Springer Nature. doi:[10.1038/ismej.2010.41](https://doi.org/10.1038/ismej.2010.41).
- Zhang, T., Barry, R., Knowles, K., Heginbottom, J., and Brown, J. 1999. Statistics and characteristics of permafrost and ground-ice distribution in the Northern Hemisphere 1. *Polar Geography* **23**: 132–154. doi:[10.1080/10889379909377670](https://doi.org/10.1080/10889379909377670).

## 6. APPENDIX

Table A.1. List of phyla that made up less than 1% of each sample and were grouped into the “Other” category.

d__Bacteria;p__Chlamydiota
d__Bacteria;p__Armatimonadota
d__Bacteria;p__Planctomycetota
d__Bacteria;p__Fibrobacterota
d__Bacteria;p__Verrucomicrobiota
d__Bacteria;p__Firmicutes_C
d__Bacteria;p__Atribacterota
d__Bacteria;p__Desulfobacterota_G_459544
d__Bacteria;p__Cyanobacteria
d__Bacteria;p__Desulfobacterota_B
d__Bacteria;p__Myxococcota_A_437813
d__Bacteria;p__UBA10199
d__Bacteria;p__Desulfobacterota_E
d__Bacteria;p__Elusimicrobiota
d__Bacteria;p__Sumerlaeota
d__Archaea;p__Nanoarchaeota
d__Bacteria;p__Firmicutes_B_370535
d__Archaea;p__Halobacteriota
d__Bacteria;p__Desulfobacterota_G_459546
d__Bacteria;p__Eisenbacteria
d__Bacteria;p__Eremiobacterota
d__Bacteria;p__Nitrospinota_B
d__Bacteria;p__Hydrogenedentota
d__Bacteria;p__Deinococcota
d__Bacteria;p__Desulfobacterota_I
d__Bacteria;p__Nitrospirota_A_437815
d__Bacteria;p__Dormibacterota
d__Bacteria;p__Firmicutes_B_370518
Unassigned;__
d__Bacteria;p__Caldisericota
d__Bacteria;p__Spirochaetota
d__Bacteria;p__FCPU426
d__Archaea;p__Thermoplasmatota
d__Bacteria;p__Methylomirabilota
d__Bacteria;p__Campylobacterota

d__Bacteria;p__Fusobacteriota
d__Bacteria;p__
d__Bacteria;p__Latescibacterota
d__Bacteria;p__WOR-3
d__Archaea;p__Methanobacteriota_A_1229
d__Bacteria;p__Firmicutes_B_370539
d__Bacteria;p__Omnitrophota
d__Bacteria;p__JdFR-76
d__Bacteria;p__Firmicutes_G
d__Bacteria;p__Ratteibacteria
d__Bacteria;p__Desulfobacterota_D
d__Bacteria;p__Deinobacteriota
d__Bacteria;p__Firmicutes_B_370541
d__Bacteria;p__Thermosulfidibacterota

Table A.2. Results of the Similarity Percentage test used to compare the permafrost microbial community composition between field sites at Time 0. The cumulative contributions of the 10 ASVs with the greatest contributions to the dissimilarity between community composition are listed.

ASV	Cumulative Contribution
d__Bacteria.p__Firmicutes_D.c__Bacilli.o__Caldalkalibacillales.f__Caldalkalibacillaceae.g__Caldalkalibacillus_362013.s__Caldalkalibacillus.thermarum	0.1477988
d__Bacteria.p__Proteobacteria.c__Alphaproteobacteria.o__Sphingomonadales.f__Sphingomonadaceae.g__Sphingomonas_L_486704.	0.2099869
d__Bacteria.p__Actinobacteriota.c__Actinomycetia.o__Actinomycetales.f__Micrococcaceae.g__Nesterenkonia.	0.2697645
d__Bacteria.p__Acidobacteriota.c__Vicinamibacteria.o__Vicinamibacterales.f__UBA2999.g__Gp6.AA45.s	0.3181809
d__Bacteria.p__Actinobacteriota.c__Thermoleophilia.o__Solirubrobacterales.f__Solirubrobacteraceae_405341.g__Solirubrobacter.	0.3663353
d__Bacteria.p__Actinobacteriota.c__Actinomycetia.o__Actinomycetales.f__Micrococcaceae.	0.4069019
d__Bacteria.p__Actinobacteriota.c__Acidimicrobiia_401430.	0.4395492
d__Bacteria.	0.4622717
d__Bacteria.p__Gemmatimonadota.c__Gemmatimonadetes.o__Gemmatimonadales.f__Gemmatimonadaceae.g__AG11.s	0.4845522
d__Bacteria.p__Chloroflexota.c__Limnocyndria.o__Limnocyndrales.f__CSP1.4.g__GWC2.73.18.s	0.5068245

Table A.3. Results of the Similarity Percentage test used to compare the active layer microbial community composition between field sites at Time 0. The cumulative contributions of the 10 ASVs with the greatest contributions to the dissimilarity between community composition are listed.

ASV	Cumulative Contribution
d_Bacteria.p_Actinobacteriota.c_Actinomycetia.o_Actinomycetales.f_Micrococcaceae.	0.1056785
d_Bacteria.p_Actinobacteriota.c_Acidimicrobiia_402965.o_UBA5794.f_UBA5794.g_SZUA.442.s_SZUA.442.sp003235475	0.2044831
d_Bacteria.p_Proteobacteria.	0.2800065
d_Bacteria.p_Actinobacteriota.c_Thermoleophilia.o_Solirubrobacteriales.f_Solirubrobacteraceae_405341.g_Solirubrobacter.	0.348098
d_Bacteria.	0.3752438
d_Bacteria.p_Actinobacteriota.	0.4009242
d_Bacteria.p_Actinobacteriota.c_Thermoleophilia.o_Gaiellales.f_Gaiellaceae.g_Gaiella.s_Gaiella.oculta	0.4252694
d_Bacteria.p_Firmicutes_D.c_Bacilli.o_Caldalkalibacillales.f_Caldalkalibacillaceae.g_Caldalkalibacillus_362013.s_Caldalkalibacillus.thermarum	0.4486967
d_Bacteria.p_Acidobacteriota.c_Vicinamibacteria.o_Vicinamibacteriales.f_UBA2999.g_WHSN01.s	0.4720562
d_Bacteria.p_Actinobacteriota.c_Acidimicrobiia_401430.	0.4932513

Table A.4. Results of the Similarity Percentage test used to compare the Long Point active layer and permafrost microbial community composition at Time 0. The cumulative contributions of the 10 ASVs with the greatest contributions to the dissimilarity between community composition are listed.

ASV	Cumulative Contribution
d_Bacteria.p_Firmicutes_D.c_Bacilli.o_Caldalkalibacillales.f_Caldalkalibacillaceae.g_Caldalkalibacillus_362013.s_Caldalkalibacillus.thermarum	0.1180651
d_Bacteria.p_Actinobacteriota.c_Actinomycetia.o_Actinomycetales.f_Micrococcaceae.g_Nesterenkonia.	0.1753489
d_Bacteria.p_Proteobacteria.	0.2221595
d_Bacteria.p_Actinobacteriota.c_Actinomycetia.o_Actinomycetales.f_Micrococcaceae.	0.2660855
d_Bacteria.p_Actinobacteriota.c_Acidimicrobiia_401430.	0.2926892
d_Bacteria.p_Proteobacteria.c_Alphaproteobacteria.o_Sphingomonadales.f_Sphingomonadaceae.g_Sphingomonas_L_486704.	0.3191567
d_Bacteria.p_Actinobacteriota.c_Thermoleophilia.o_Solirubrobacteriales.f_Solirubrobacteraceae_405341.g_Solirubrobacter.	0.3448264
d_Bacteria.	0.3688617
d_Bacteria.p_Actinobacteriota.	0.3917538

d_Bacteria.p__Chloroflexota.c__Limnocyndria.o__Limnocyndrales.f__CSP1.4.g__GWC2.73.18.s	0.4141886
---	-----------

Table A.5. Results of the Similarity Percentage test used to compare the Augustus Hills active layer and permafrost microbial community composition at Time 0. The cumulative contributions of the 10 ASVs with the greatest contributions to the dissimilarity between community composition are listed.

ASV	Cumulative Contribution
d_Bacteria.p__Firmicutes_D.c__Bacilli.o__Caldalkalibacillales.f__Caldalkalibacillaceae.g__Caldalkalibacillus_362013.s__Caldalkalibacillus.thermarum	0.1604161
d_Bacteria.p__Actinobacteriota.c__Actinomycetia.o__Actinomycetales.f__Micrococcaceae.	0.2298979
d_Bacteria.p__Actinobacteriota.c__Acidimicrobiia_402965.o__UBA5794.f__UBA5794.g__SZUA.442.s__SZUA.442.sp003235475	0.2955799
d_Bacteria.p__Proteobacteria.c__Alphaproteobacteria.o__Sphingomonadales.f__Sphingomonadaceae.g__Sphingomonas_L_486704.	0.3567588
d_Bacteria.p__Actinobacteriota.c__Actinomycetia.o__Actinomycetales.f__Micrococcaceae.g__Nesterenkonia.	0.4133969
d_Bacteria.p__Proteobacteria.	0.4545391
d_Bacteria.p__Acidobacteriota.c__Vicinamibacteria.o__Vicinamibacterales.f__UBA2999.g__Gp6.AA45.s	0.4933258
d_Bacteria.p__Actinobacteriota.c__Acidimicrobiia_401430.	0.5219334
d_Bacteria.p__Firmicutes_D.c__Bacilli.o__Bacillales_D_310495.f__Amphibacillaceae.g__Ornithinibacillus_287146.	0.5441932
d_Bacteria.p__Actinobacteriota.c__Acidimicrobiia_401430.o__Acidimicrobiales.	0.5660178

Table A.6. Results of the Similarity Percentage test used to compare the Time 0 and post-thaw Long Point AS community compositions. The cumulative contributions of the 10 ASVs with the greatest contributions to the dissimilarity between community composition are listed.

ASV	Cumulative Contribution
d_Bacteria.p__Proteobacteria.	0.09551975
d_Bacteria.p__Actinobacteriota.c__Thermoleophilia.o__Solirubrobacterales.f__Solirubrobacteraceae_405341.	0.1789978
d_Bacteria.p__Actinobacteriota.c__Thermoleophilia.o__Solirubrobacterales.f__Solirubrobacteraceae_405341.g__Solirubrobacter.	0.23831794
d_Bacteria.p__Actinobacteriota.c__Actinomycetia.o__Actinomycetales.f__Micrococcaceae.	0.27467231
d_Bacteria.	0.30872264
d_Bacteria.p__Chloroflexota.	0.33913926
d_Bacteria.p__Actinobacteriota.c__Thermoleophilia.o__Solirubrobacterales.	0.3605117
d_Bacteria.p__Actinobacteriota.	0.38094992

d_Bacteria.p_Actinobacteriota.c_Thermoleophilia.o_Gaiellales.f_Gaiellaceae.g_Gaiella.s_Gaiella.occulta	0.40010431
d_Bacteria.p_Proteobacteria.c_Alphaproteobacteria.o_Sphingomonadales.f_Sphingomonadaceae.g_Sphingorhabdus B 483718.s	0.41906956

Table A.7. Results of the Similarity Percentage test used to compare the Time 0 and post-thaw Long Point AS+PM community compositions. The cumulative contributions of the 10 ASVs with the greatest contributions to the dissimilarity between community composition are listed.

ASV	Cumulative Contribution
d_Bacteria.p_Proteobacteria. . . . .	0.1024831
d_Bacteria.p_Actinobacteriota.c_Thermoleophilia.o_Solirubrobacterales.f_Solirubrobacteraceae 405341. .	0.1556206
d_Bacteria. . . . .	0.1942362
d_Bacteria.p_Chloroflexota. . . . .	0.2327192
d_Bacteria.p_Chloroflexota.c_Limnocyndria.o_Limnocyndrales.f_CSP1.4.g_GWC2.73.18.s	0.2697501
d_Bacteria.p_Firmicutes_D.c_Bacilli.o_Caldalkalibacillales.f_Caldalkalibacillaceae.g_Caldalkalibacillus_362013.s_Caldalkalibacillus.thermarum	0.3052711
d_Bacteria.p_Actinobacteriota. . . . .	0.3354098
d_Bacteria.p_Actinobacteriota.c_Actinomycetia.o_Actinomycetales.f_Micrococcaceae. .	0.3623157
d_Bacteria.p_Actinobacteriota.c_Thermoleophilia.o_Solirubrobacterales.f_Solirubrobacteraceae 405341.g_Solirubrobacter.	0.3878385
d_Bacteria.p_Gemmatimonadota.c_Gemmatimonadetes.o_Gemmatimonadales.f_GWC2.71.9. .	0.4122491

Table A.8. Results of the Similarity Percentage test used to compare the Time 0 and post-thaw Long Point AS+PN community compositions. The cumulative contributions of the 10 ASVs with the greatest contributions to the dissimilarity between community composition are listed.

ASV	Cumulative Contribution
d_Bacteria.p_Proteobacteria. . . . .	0.1147519
d_Bacteria.p_Actinobacteriota.c_Thermoleophilia.o_Solirubrobacterales.f_Solirubrobacteraceae 405341. .	0.1895065
d_Bacteria.p_Actinobacteriota.c_Thermoleophilia.o_Solirubrobacterales.f_Solirubrobacteraceae 405341.g_Solirubrobacter.	0.247426
d_Bacteria.p_Actinobacteriota.c_Actinomycetia.o_Actinomycetales.f_Micrococcaceae. .	0.2941072
d_Bacteria.p_Chloroflexota. . . . .	0.3257036
d_Bacteria.p_Bacteroidota.c_Bacteroidia.o_Flavobacteriales_877923.f_Flavobacteriaceae.g_Flavobacterium.	0.3507222
d_Bacteria. . . . .	0.3727583
d_Bacteria.p_Actinobacteriota.c_Thermoleophilia.o_Solirubrobacterales. . . . .	0.3937353

d_Bacteria.p_Gemmatimonadota.c_Gemmatimonadetes.o_Gemmatimonadales.f_GWC2.71.9.g_JABFSM01.s_JABFSM01.sp009692115	0.4147068
d_Bacteria.p_Gemmatimonadota.c_Gemmatimonadetes.o_Gemmatimonadales.f_GWC2.71.9.	0.4335264

Table A.9. Results of the Similarity Percentage test used to compare the Time 0 and post-thaw Long Point AS+PM+PN community compositions. The cumulative contributions of the 10 ASVs with the greatest contributions to the dissimilarity between community composition are listed.

ASV	Cumulative Contribution
d_Bacteria.p_Actinobacteriota.c_Actinomycetia.o_Actinomycetales.f_Micrococcaceae.	0.04746714
d_Bacteria.p_Firmicutes_D.c_Bacilli.o_Caldalkalibacillales.f_Caldalkalibacillaceae.g_Caldalkalibacillus_362013.s_Caldalkalibacillus.thermarum	0.09243371
d_Bacteria.p_Actinobacteriota.c_Thermoleophilia.o_Solirubrobacteriales.f_Solirubrobacteraceae_405341.	0.13390385
d_Bacteria.p_Actinobacteriota.c_Thermoleophilia.o_Solirubrobacteriales.f_Solirubrobacteraceae_405341.g_Solirubrobacter.	0.17308134
d_Bacteria.p_Chloroflexota.	0.21218223
d_Bacteria.p_Chloroflexota.c_Limnocyndria.o_Limnocyndrales.f_CSP1.4.g_GWC2.73.18.s	0.24777028
d_Bacteria.p_Actinobacteriota.	0.27855415
d_Bacteria.p_Proteobacteria.	0.30798652
d_Bacteria.p_Gemmatimonadota.c_Gemmatimonadetes.o_Gemmatimonadales.f_GWC2.71.9.	0.33403189
d_Bacteria.	0.35683253

Table A.10. Results of the Similarity Percentage test used to compare the Time 0 and post-thaw Long Point PS+AM community compositions. The cumulative contributions of the 10 ASVs with the greatest contributions to the dissimilarity between community composition are listed.

ASV	Cumulative Contribution
d_Bacteria.p_Firmicutes_D.c_Bacilli.o_Caldalkalibacillales.f_Caldalkalibacillaceae.g_Caldalkalibacillus_362013.s_Caldalkalibacillus.thermarum	0.08170175
d_Bacteria.p_Actinobacteriota.c_Actinomycetia.o_Actinomycetales.f_Micrococcaceae.	0.13658684
d_Bacteria.p_Proteobacteria.	0.1902429
d_Bacteria.p_Actinobacteriota.c_Thermoleophilia.o_Solirubrobacteriales.f_Solirubrobacteraceae_405341.g_Solirubrobacter.	0.21823737
d_Bacteria.p_Proteobacteria.c_Alphaproteobacteria.o_Sphingomonadales.f_Sphingomonadaceae.g_Sphingomonas_L_486704.	0.2458051
d_Bacteria.p_Actinobacteriota.c_Acidimicrobiia_401430.	0.26927038
d_Bacteria.p_Acidobacteriota.c_Vicinamibacteria.o_Vicinamibacteriales.f_UBA2999.g_WHSN01.s	0.29239427

d_Bacteria. . . . .	0.31221799
d_Bacteria.p_Chloroflexota.c_Limnocyndria.o_Limnocyndrales.f_CSP1.4.g_GWC2.73.18.s	0.33163773
d_Bacteria.p_Acidobacteriota.c_Vicinamibacteria.o_Vicinamibacterales.f_UBA2999.g.s	0.35035192

Table A.11. Results of the Similarity Percentage test used to compare the Time 0 and post-thaw Long Point PS+AM+AN community compositions. The cumulative contributions of the 10 ASVs with the greatest contributions to the dissimilarity between community composition are listed.

ASV	Cumulative Contribution
d_Bacteria.p_Actinobacteriota.c_Actinomycetia.o_Actinomycetales.f_Micrococcaceae. .	0.08167732
d_Bacteria.p_Proteobacteria. . . . .	0.15564504
d_Bacteria.p_Firmicutes_D.c_Bacilli.o_Caldalkalibacillales.f_Caldalkalibacillaceae.g_Caldalkalibacillus_362013.s_Caldalkalibacillus.thermarum	0.21967376
d_Bacteria.p_Actinobacteriota.c_Thermoleophilia.o_Solirubrobacterales.f_Solirubrobacteraceae_405341.g_Solirubrobacter.	0.24528874
d_Bacteria.p_Proteobacteria.c_Alphaproteobacteria.o_Sphingomonadales.f_Sphingomonadaceae.g_Sphingomonas_L_486704.	0.26957308
d_Bacteria.p_Actinobacteriota.c_Acidimicrobiia_401430. . . .	0.2913537
d_Bacteria. . . . .	0.3098894
d_Bacteria.p_Actinobacteriota. . . . .	0.32822084
d_Bacteria.p_Gemmatimonadota.c_Gemmatimonadetes.o_Gemmatimonadales.f_Gemmatimonadaceae.g_AG11.s	0.34617293
d_Bacteria.p_Actinobacteriota.c_Acidimicrobiia_401430.o_Acidimicrobiales. . .	0.36372231

Table A.12. Results of the Similarity Percentage test used to compare the Time 0 and post-thaw Augustus Hills AS community compositions. The cumulative contributions of the 10 ASVs with the greatest contributions to the dissimilarity between community composition are listed.

ASV	Cumulative Contribution
d_Bacteria.p_Actinobacteriota.c_Actinomycetia.o_Actinomycetales.f_Micrococcaceae. .	0.1193868
d_Bacteria.p_Firmicutes_D.c_Bacilli.o_Caldalkalibacillales.f_Caldalkalibacillaceae.g_Caldalkalibacillus_362013.s_Caldalkalibacillus.thermarum	0.2090158
d_Bacteria.p_Proteobacteria. . . . .	0.271287
d_Bacteria.p_Actinobacteriota.c_Acidimicrobiia_402965.o_UBA5794.f_UBA5794.g_SZUA.442.s_SZUA.442.sp003235475	0.3316027
d_Bacteria.p_Proteobacteria.c_Gammaproteobacteria.o_Xanthomonadales_616009.f_Xanthomonadaceae_616009.g_Arenimonas_613591.s_Arenimonas.oryziterrae	0.370803

d_Bacteria.p__Proteobacteria.c__Gammaproteobacteria.o__Xanthomonadales_616009.f__Xanthomonadaceae_616009.g__Arenimonas_613591.s__Arenimonas.metalli	0.4030942
d_Bacteria.p__Actinobacteriota.c__Acidimicrobiia_401430. . . .	0.4327065
d_Bacteria.p__Acidobacteriota.c__Vicinamibacteria.o__Vicinamibacterales.f__SCN.69.37.g__SCN.69.37.s	0.4602219
d_Bacteria.p__Proteobacteria.c__Alphaproteobacteria.o__Sphingomonadales.f__Sphingomonadaceae. .	0.4843191
d_Bacteria.p__Actinobacteriota.c__Acidimicrobiia_401430.o__Acidimicrobiales. . . .	0.5063677

Table A.13. Results of the Similarity Percentage test used to compare the Time 0 and post-thaw Augustus Hills AS+PN community compositions. The cumulative contributions of the 10 ASVs with the greatest contributions to the dissimilarity between community composition are listed.

ASV	Cumulative Contribution
d_Bacteria.p__Actinobacteriota.c__Actinomycetia.o__Actinomycetales.f__Micrococcaceae. .	0.1239785
d_Bacteria.p__Acidobacteriota.c__Vicinamibacteria.o__Vicinamibacterales.f__SCN.69.37.g__SCN.69.37.s	0.2475976
d_Bacteria.p__Firmicutes_D.c__Bacilli.o__Caldalkalibacillales.f__Caldalkalibacillaceae.g__Caldalkalibacillus_362013.s__Caldalkalibacillus.thermarum	0.320389
d_Bacteria.p__Proteobacteria.c__Gammaproteobacteria.o__Xanthomonadales_616009.f__Xanthomonadaceae_616009.g__Arenimonas_613591.s__Arenimonas.oryziterrae	0.385376
d_Bacteria.p__Actinobacteriota.c__Acidimicrobiia_402965.o__UBA5794.f__UBA5794.g__SZUA.442.s__SZUA.442.sp003235475	0.4395434
d_Bacteria.p__Proteobacteria. . . . .	0.4899767
d_Bacteria. . . . .	0.5219252
d_Bacteria.p__Actinobacteriota.c__Acidimicrobiia_401430. . . . .	0.5460924
d_Bacteria.p__Actinobacteriota.c__Acidimicrobiia_401430.o__Acidimicrobiales. . . .	0.5673952
d_Bacteria.p__Gemmatimonadota.c__Gemmatimonadetes.o__Gemmatimonadales.f__Gemmatimonadaceae.g__AG11.s	0.5872059

Table A.14. Results of the Similarity Percentage test used to compare the Time 0 and post-thaw Augustus Hills AS+PM community compositions. The cumulative contributions of the 10 ASVs with the greatest contributions to the dissimilarity between community composition are listed.

ASV	Cumulative Contribution
d_Bacteria.p__Firmicutes_D.c__Bacilli.o__Caldalkalibacillales.f__Caldalkalibacillaceae.g__Caldalkalibacillus_362013.s__Caldalkalibacillus.thermarum	0.100155
d_Bacteria.p__Actinobacteriota.c__Acidimicrobiia_402965.o__UBA5794.f__UBA5794.g__SZUA.442.s__SZUA.442.sp003235475	0.1748885

d_Bacteria.p_Actinobacteriota.c_Actinomycetia.o_Actinomycetales.f_Micrococcaceae.	0.2472121
d_Bacteria.p_Proteobacteria.	0.3052185
d_Bacteria.p_Proteobacteria.c_Alphaproteobacteria.o_Sphingomonadales.f_Sphingomonadaceae.g_Sphingomonas_L_486704.	0.3463796
d_Bacteria.p_Acidobacteriota.c_Vicinamibacteria.o_Vicinamibacteriales.f_SCN.69.37.g_SCN.69.37.s	0.3850788
d_Bacteria.p_Proteobacteria.c_Gammaproteobacteria.o_Xanthomonadales_616009.f_Xanthomonadaceae_616009.g_Arenimonas_613591.s_Arenimonas.oryziterrae	0.4199223
d_Bacteria.p_Gemmatimonadota.c_Gemmatimonadetes.o_Gemmatimonadales.f_Gemmatimonadaceae.g_AG11.s	0.4544587
d_Bacteria.p_Acidobacteriota.c_Vicinamibacteria.o_Vicinamibacteriales.f_UBA2999.g_Gp6.AA45.s	0.4833626
d_Bacteria.p_Actinobacteriota.c_Actinomycetia.o_Actinomycetales.f_Micrococcaceae.g_Nesterenkonia.	0.5051315

Table A.15. Results of the Similarity Percentage test used to compare the Time 0 and post-thaw Augustus Hills AS+PM+PN community compositions. The cumulative contributions of the 10 ASVs with the greatest contributions to the dissimilarity between community composition are listed.

ASV	Cumulative Contribution
d_Bacteria.p_Firmicutes_D.c_Bacilli.o_Caldalkalibacillales.f_Caldalkalibacillaceae.g_Caldalkalibacillus_362013.s_Caldalkalibacillus.thermarum	0.1176941
d_Bacteria.p_Actinobacteriota.c_Acidimicrobiia_402965.o_UBA5794.f_UBA5794.g_SZUA.442.s_SZUA.442.sp003235475	0.1876473
d_Bacteria.p_Actinobacteriota.c_Actinomycetia.o_Actinomycetales.f_Micrococcaceae.	0.2462336
d_Bacteria.p_Proteobacteria.	0.3016567
d_Bacteria.p_Acidobacteriota.c_Vicinamibacteria.o_Vicinamibacteriales.f_SCN.69.37.g_SCN.69.37.s	0.3407351
d_Bacteria.p_Proteobacteria.c_Alphaproteobacteria.o_Sphingomonadales.f_Sphingomonadaceae.g_Sphingomonas_L_486704.	0.3762192
d_Bacteria.p_Acidobacteriota.c_Vicinamibacteria.o_Vicinamibacteriales.f_UBA2999.g_Gp6.AA45.s	0.4106605
d_Bacteria.p_Actinobacteriota.c_Actinomycetia.o_Actinomycetales.f_Micrococcaceae.g_Nesterenkonia.	0.4344093
d_Bacteria.p_Firmicutes_D.c_Bacilli.o_Bacillales_H.f_Bacillaceae_D_361234.g_Bacillus_M.s_Bacillus_M.halodurans	0.4559751
d_Bacteria.p_Actinobacteriota.c_Acidimicrobiia_401430.	0.4770055

Table A.16. Results of the Similarity Percentage test used to compare the Time 0 and post-thaw Augustus Hills PS community compositions. The cumulative contributions of the 6 ASVs with the greatest contributions to the dissimilarity between community composition are listed.

ASV	Cumulative Contribution
d_Bacteria.p__Acidobacteriota.c__Vicinamibacteria.o__Vicinamibacteriales.f__UBA2999.g__Gp6.AA45.s	0.290196
d_Bacteria.p__Gemmatimonadota.c__Gemmatimonadetes.o__Gemmatimonadales.f__Gemmatimonadaceae.g__AG11.s	0.4180625
d_Bacteria.p__Firmicutes_D.c__Bacilli.o__Caldalkalibacillales.f__Caldalkalibacillaceae.g__Caldalkalibacillus_362013.s__Caldalkalibacillus.thermarum	0.5397148
d_Bacteria.p__Actinobacteriota.c__Actinomycetia.o__Actinomycetales.f__Micrococcaceae.	0.6059662
d_Bacteria.p__Proteobacteria.c__Alphaproteobacteria.o__Sphingomonadales.f__Sphingomonadaceae.g__Sphingomonas_L_486704.	0.6692239
d_Bacteria.p__Actinobacteriota.c__Actinomycetia.o__Actinomycetales.f__Micrococcaceae.g__Nesterenkonia.	0.7317876

Table A.17. Results of the Similarity Percentage test used to compare the Time 0 and post-thaw Augustus Hills PS+AN community compositions. The cumulative contributions of the 5 ASVs with the greatest contributions to the dissimilarity between community composition are listed.

ASV	Cumulative Contribution
d_Bacteria.p__Acidobacteriota.c__Vicinamibacteria.o__Vicinamibacteriales.f__UBA2999.g__Gp6.AA45.s	0.3420592
d_Bacteria.p__Firmicutes_D.c__Bacilli.o__Caldalkalibacillales.f__Caldalkalibacillaceae.g__Caldalkalibacillus_362013.s__Caldalkalibacillus.thermarum	0.4873376
d_Bacteria.p__Gemmatimonadota.c__Gemmatimonadetes.o__Gemmatimonadales.f__Gemmatimonadaceae.g__AG11.s	0.6146612
d_Bacteria.p__Proteobacteria.c__Alphaproteobacteria.o__Sphingomonadales.f__Sphingomonadaceae.g__Sphingomonas_L_486704.	0.6761142
d_Bacteria.p__Actinobacteriota.c__Actinomycetia.o__Actinomycetales.f__Micrococcaceae.g__Nesterenkonia.	0.737447

Table A.18. Results of the Similarity Percentage test used to compare the Time 0 and post-thaw Augustus Hills PS+AM+AN community compositions. The cumulative contributions of the 7 ASVs with the greatest contributions to the dissimilarity between community composition are listed.

ASV	Cumulative Contribution
d_Bacteria.p__Acidobacteriota.c__Vicinamibacteria.o__Vicinamibacteriales.f__UBA2999.g__Gp6.AA45.s	0.2842427

d_Bacteria.p_Firmicutes_D.c_Bacilli.o_Caldalkalibacillales.f_Caldalkalibacillaceae.g_Caldalkalibacillus_362013.s_Caldalkalibacillus.thermarum	0.4270447
d_Bacteria.p_Gemmatimonadota.c_Gemmatimonadetes.o_Gemmatimonadales.f_Gemmatimonadaceae.g_AG11.s	0.5071134
d_Bacteria.p_Actinobacteriota.c_Actinomycetia.o_Actinomycetales.f_Micrococcaceae.	0.5741061
d_Bacteria.p_Proteobacteria.c_Alphaproteobacteria.o_Sphingomonadales.f_Sphingomonadaceae.g_Sphingomonas_L_486704.	0.6351492
d_Bacteria.p_Actinobacteriota.c_Actinomycetia.o_Actinomycetales.f_Micrococcaceae.g_Nesterenkonia.	0.6858755
d_Bacteria.p_Proteobacteria.c_Alphaproteobacteria.o_Rhizobiales_A_504705.f_Beijerinckiaceae.g_Methylobacterium.s_Methylobacterium.komagatae	0.7111384

Table A.19. Results of the Similarity Percentage test used to compare the Time 0 and post-thaw Augustus Hills PS+AM community compositions. The cumulative contributions of the 8 ASVs with the greatest contributions to the dissimilarity between community composition are listed.

<b>ASV</b>	<b>Cumulative Contribution</b>
d_Bacteria.p_Acidobacteriota.c_Vicinamibacteria.o_Vicinamibacteriales.f_UBA2999.g_Gp6.AA45.s	0.2601069
d_Bacteria.p_Firmicutes_D.c_Bacilli.o_Caldalkalibacillales.f_Caldalkalibacillaceae.g_Caldalkalibacillus_362013.s_Caldalkalibacillus.thermarum	0.3882729
d_Bacteria.p_Actinobacteriota.c_Actinomycetia.o_Actinomycetales.f_Micrococcaceae.	0.4745068
d_Bacteria.p_Gemmatimonadota.c_Gemmatimonadetes.o_Gemmatimonadales.f_Gemmatimonadaceae.g_AG11.s	0.5582002
d_Bacteria.p_Proteobacteria.c_Alphaproteobacteria.o_Sphingomonadales.f_Sphingomonadaceae.g_Sphingomonas_L_486704.	0.6166703
d_Bacteria.p_Actinobacteriota.c_Actinomycetia.o_Actinomycetales.f_Micrococcaceae.g_Nesterenkonia.	0.6688967
d_Bacteria.p_Proteobacteria.	0.6975311
d_Bacteria.p_Firmicutes_D.c_Bacilli.o_Bacillales_H.f_Bacillaceae_D_361234.g_Bacillus_M.s_Bacillus_M.halodurans	0.7213215